แสดงให้เห็นถึงการจัดเรียงตัวกันของไอออนแคลเซียมในโพรงของกลุ่มก้อนแอมโมเนียอีกด้วย การ เกิดกลุ่มก้อนของแอมโมเนีย การลอยตัวของไอออนแคลเซียมในโพรงของแอมโมเนียตลอดถึงการจัด เรียงตัวของไอออน สามารถเห็นได้จากภาพสเตริโอแกรมที่สุ่มมาจากคอนฟิกุเรชันที่ได้จากการซิมุเลชัน รูปที่ 3.18 และภาพที่เลือกมาเมื่อพบว่าไอออนแคลเซียมเรียงตัวกันเป็นแนวเส้น ดังรูปที่ 3.20

ข้อมูลจากฟังก์ชันการกระจายของมุม Ca(II)-Ca(II)-Ca(II) ในรูปที่ 3.19 แสดงถึง ความหนาแน่นที่สูงที่มุมประมาณ 180 และ 130 องศา ซึ่งทำให้คาดได้ว่าน่าจะมีไอออนของแคลเจียมที่ เรียงตัวต่อเนื่องกันเป็นแถวยาวดังที่กล่าวข้างต้น รายละเอียดเพิ่มเติมสามารถดูได้ในเอกสารอ้างอิง

เอกสารอ้างอิง

- 1. Thomson, J. C. 1976, Electron in Liquid Ammonia, Clarendon Press, Oxford.
- 2. Metal Ammonia Solutions, Colloque Weyl I, edited by Lepoutre, G. and Spienko, M. J. (Benjamin, New York, 1964).
- 3. Metal Ammonia Solutions, Colloque Weyl II, edited by Lagowski, J. J. and Spienko, M. J. (Butterworths, London 1970).
- 4. Electron in Fluids, Colloque Weyl III, edited by Jortner, J. and Kesner, N. R.. (Springer, New York, 1973).
- 5 *J. Phys. Chem.* **79,** 2789 (1975) and references therein.
- 6. J. Phys. Chem. 84, 1065 (1980) and references therein.
- 7. J. Phys. Chem. 88, 3699 (1984) and references therein.
- 8. In Proceedings of the International Conference on Metal in Solutions,
 Colloque Weyl VII, France, June, 1991.
- 9. Hannongbua, S., Ishida, T., Spohr, E. and Heinzinger, K. 1988, Z. Naturforsch.

 43a, 572.
- 10. Hannongbua, S. and Kokpol, S. U. 1992, Inorg. Chim. Acta 202, 85.
- 11. Kheawsrikul, S., Hannongbua, S. and Rode, B. M. 1991, Z. Naturforsch. 46a, 111.
- 12. Hannongbua, S. and Rode, B. M. 1992, Chem. Phys. 162, 257.
- 13. Hannongbua, S., Kerdcharoen, T. and Rode, B. M. 1992, J. Chem. Phys. 96, 6945.
- 14. Gurskii, Z., Hannongbua, S. and Heinzinger, K. 1993, Mol. Phys. 78, 461.
- 15. Gurskii, Z., Kushaba, V., Hannongbua, S., and Heinzinger, K. 1995

 J. Met. Phys. Adv. Tech., 17, 62.
- 16. Impey, R. W., Sprik, M. and Klein, M. L. 1987, J. Am. Chem. Soc. 109, 5900.
- 17. ตัวอย่างเช่น Computer Simulation of Liquids, edited by Allen, M. P. and Tildesley, D. J. (Oxford University Press, New York 1987).
- 18. ตัวอย่างเช่น Ab-initio Molecular Orbital Theory, edited by Hehre, W. J., Radom.
 L., Schleyer, P. R. and Pople, J.A. (John Wiley & Sons, New York, 1986).
- 19 Narten, A. H. 1977, J. Chem. Phys. 66, 3117.
- 20 ตัวอย่างเช่น Duguette, A., Ellis, K. H., Watts, W. and Klein, M. L. 1987.

 J. Chem. Phys. 68, 2544
- 21 Martyna, G. J. and Klein, M. L. 1991, J. Plys. Chem., 95, 515.

- 22. Sagarik, K. P., Ahlrichs, P. and Brode, S. 1986, Mol. Phys., 57, 1247.
- 23. Impey, R. W. and Klein, M. L. 1984, Chem. Phys. Lett., 104, 579.
- 24. Jorgensen, W. L. and Ibrahim, M. 1980, J. Am. Chem. Soc., 102, 3309.
- 25. Kheawsrikul, S., Hannongbua, S., Kokpol, S. U. and Rode, B. M. 1989, J. Chem. Soc. Faraday Trans. II, 85, 643.
- 26. ตัวอย่างเช่น Clementi, E., Kistenmacher, H., Kolos, W. and Romano, S. 1980, J. Phys. Chem., 61, 799.
- 27 Benedict, W. S. and Plyler, E. K. 1985, Can. J. Phys., 35, 890.
- 28 Mulliken, R. S. 1955, J. Chem. Phys., 23, 1833, 1841, 2338, 2343.
- 29. Harrion, W. A. 1966 Pseudopotentials in the Theory of Metal (Benjamin).
- 30. Gurskii, Z. and Heinzinger H. 1988, Preprint ITP, 88-49E (Institute for Theoretical Physics, Kiev).
- 31. Gurskii, Z., Heinzinger H. and Saban, A. 1990, Preprint ITP, 90-55E (Institute for Theoretical Physics, Kiev).
- 32. Ishimaru, S. and Utsumi, K. 1981, Phys. Rev., B24, 7385.
- 33. Johnson, W. C., Meyer, A. W. and Martens, R. D. 1950, J. Am. Chem. Soc., 72, 1842.
- 34. Sidhisoradei, W., Hannongbua, S. and Ruffolo, D. 1998, Z. Naturforsch., 53a, 208.
- 35. ตัวอย่างเช่น เอกสารหมายเลข 9,16, 22-24.
- 36 Lybrand, T. P and Kollman, P. A. 1985, J. Chem. Phys. 88, 2923.
- Ortega-Blake, I., Hemandez, J. and Novaro, m O. 1984, J. Chem. Phys. 81, 1894.
- 38. Clementi, E., Kistenmacher, H., Kolos, W. and Romano, S. 1980 Theor. Chim. Acta 55, 257.
- 39. Kistenmacher, H., Popkie, H. and Clementi, E. 1974 J. Chem. Phys. 61, 799.
- 40. Kochanski, E. 1987 Chem. Phys. Lett. 132, 143.
- 41. Hannongbua, S. 1997 J. Chem. Phys. 106, 6076.
- 42. Dunning, T. H. 1970, J. Chem. Phys., 63, 2823.
- 43. Hannongbua, S. 1998 Chem. Phys. Lett. 288, 663.
- 44. Hannongbua, S. submitted for publication (J. Am. Chem. Soc.).
- Hannongbua, S., Kokpol, S.U., Gurskii, Z., and Heinzinger, K., Z.Naturforsch. 52a, 828 (1997).

ภาคผนวก

Output จากโครงการฯ

บทความวิจัย ที่ลงพิมพ์แล้ว 3 เรื่อง คือ

- 1. Hannongbua, S., Kokpol, S.U., Gurskii, Z., and Heinzinger, K., Cluster Structure of Concentrated Lithium-Liquid Ammonia Solutions: A Monte Carlo Study, Z.Naturforsch. 52a, 828 (1997).
- 2. Hannongbua, S. On the Solvation of Lithium Ion in Liquid Ammonia: Monte Carlo Simulations with a Three-body Potential, Chem. Phys. Lett., 288, 663 (1998).
- 3. Sidhisoradej, W., Ruffolo, D. and Hannongbua, S. Three-body Effects in Calcium(II)-Ammonia Solution: Molecular Dynamics Simulations. Z.Naturforsch. 53a, 756 (1998).

Manuscript ที่อยู่ระหว่างการส่งลงพิมพ์ 1 เรื่องคือ

1. Hannongbua, S. The best structural data of Liquid Ammonia based on the Pair Approximation: the first Principle Monte Carlo Simulation submitted for publication (J. Am. Chem. Soc.).

Cluster Formation in a Concentrated Lithium-Liquid Ammonia Solution. A Monte Carlo Study

- S. Hannongbua*, S. Kokpol*, Z. Gurskiib, and K. Heinzinger's
- * Department of Chemistry, Faculty of Science, Chulalongkorn University, Bangkok 10330, Thailand
- Institute for Condensed Matter Physics, Ukrainian Academy of Sciences, Lviv 290005, Ukrainia
 Max-Planck-Institut für Chemie (Otto-Hahn-Institut), P.O.B. 3060, D-55020 Main.
- Z. Naturforsch. 52a, 828-834 (1997), received October 13, 1997

Results of a Monte Carlo study of a lithium-figured ammonia solution at 240 K are reported. The basic cube contained 135 Li* and 1025 NH₃. With an experimental density of 0.554 g cm³ a side length of 37.89 Å resulted. The pseudopotential theory is employed, which permits the exclusion of the electrons from an explicit consideration. The structure of the solution is described by various site-site radial distribution functions. The six ammonia molecules in the first solvation shell of the lithium ion are arranged octahedrally. Clusters are formed which consist almost exclusively of two solvated Li* which have simultaneously either one ammonia molecule or an octahedral edge of acoetahedral plane in common. About one third of the ammonia molecules belong to the bulk phase

1. Introduction

In [1] an approach has been suggested for the investigation by computer simulation of systems which contain free electrons. Through the application of the pseudopotential theory, renormalized effective interatomic potentials are derived through which electrons can be excluded from explicite consideration and classical computer simulation methods can be employed. The usefulness of this method has been demonstrated by the calculation of structural properties of concentrated metal ammonia solutions. Preliminary results have been presented for two different concentrations with lithium mole fractions $x_{11} = 0.118$ and 0.1958.

Although metal ammonia solutions are of great interest from various points of view, there is a serious lack of information on their structural and dynamical properties because of experimental difficulties. Computer simulations cannot only fill this gap but can additionally contribute to a better understanding of the macroscopic properties of such systems on a molecular level.

During the course of the simulations of the lithium ammonia solutions with the potentials reported in [1], we realized that an improvement of both contributions – the direct and indirect ones – to the total potential

$$V_{\text{rot}}^{ij}(R) = V_{\text{rod}}^{ij}(R) + V_{\text{dia}}^{ij}(R)$$
 (1)

Reprint (quests to Dr. K. Heinzinger

is needed. For the improvement of Γ_{ij} (E) new are initio calculations have been performed and during the newly performed fitting procedure the charges were not considered to be free parameters. It could be shown that it is a unique feature of metal ammonia solutions that indirect contributions are not only functions of metal concentration but also of temperature [2]. With the new potential, a Monte Carlo (MC) simulation of a lithium-hquid ammonia solution with a lithium mole fraction $x_{1,i} = 0.1164$ has been performed.

In the next section the improved potential will be presented, and details of the simulation will be given. The structure of the solution will be discussed in the following section on the basis of radial distribution functions, the orientation of the ammonia molecules their geometrical arrangement in the solvation shells of the ions, and the formation of cluster, consisting of solvated lithium ions.

2. Potential Functions and Details of the Simulation

A rigid ammonia model is employed in the simulation with an N-H distance of 1.0124 Å and an N-H-N angle of 106.67. [3] The partial charges of 0.2674 [e] and = 0.8022 [e] on the hydrogen and the intropen atoms respectively, are taken from SC1 calculations of the ammonia molecule [4].

The direct ammonia animonia potential is the same as described in [8] while the lithium lemnorabilities of

lithium-lithium potentials have been newly derived from ab initio calculations using the DZP basis set of Dunning [6] and the HONDO 7 program [7]. They are presented now by

$$V_{\text{LiN}}(R) = -\frac{1115}{R} - \frac{3516}{R^4} + 120417 \exp(-3.31 R), (2a)$$

$$V_{LiH}(R) = \frac{372}{R} + \frac{49.31}{R^4} + 2241 \exp(-2.61 R),$$
 (2b)

$$V_{\text{LiLi}}(R) = \frac{1390}{R} - 18.71 \exp(-1.62 R),$$
 (2c)

where the energies are given in kJ/mol and R in Å.

The indirect interaction as a function of the interatomic distance, R, can be derived from the Fourier transformation of the model pseudopotential, $w_i(q)$, where i, j = H, N and Li⁺:

$$V_{\text{ind}}^{ij}(R) = \frac{\Omega}{\pi^2} \int_0^\infty F_{ij}(q) \frac{\sin q R}{R} q dq$$
 (3)

with

$$F_{ij}(q) = \frac{\Omega q^2}{8 \pi} w_i(q) \frac{1 - \varepsilon(q)}{\varepsilon(q)} w_j(q), \tag{4}$$

where

$$w_{i}(q) = -\frac{4 \pi z_{i}}{\Omega q^{2}} \cos(q r_{c,i})$$
 (5)

and the dielectric function

$$\varepsilon(q) = 1 + \frac{4\pi}{q^2} \Pi(q) \tag{6}$$

with

$$\Pi(q) = \frac{k_F}{\pi^2} \frac{f(x)}{1 - (4\mu^2/x^2) G(x) f(x)}$$
(7)

and

$$x = \frac{q}{k_F}, \quad \mu^2 = \frac{1}{\pi k_F}, \quad k_F = \left(\frac{3 \pi^2 z_m N_m}{\Omega}\right)^{1/3},$$
 (8)

$$f(x) = \frac{1}{2} + \frac{4 - x^2}{8x} \ln \left| \frac{2 + x}{2 - x} \right|, \tag{9}$$

$$z_{\rm N} = -0.8022, \quad z_{\rm H} = 0.2674, \quad z_{\rm H} = 1.0.$$
 (10)

The effective radii of the ions were chosen to be

$$r_{c,N} = 1.51, \quad r_{c,B} = 0.0, \quad r_{c,Li} = 1.28.$$
 (11)

 Ω is the volume of the system, $N_{\rm Li}$ and $z_{\rm Li}$ are the number of metal ions and their charges, respectively. For further details the reader is referred to [1].

In the course of our investigations we realized that, different from pure metals, in metal-ammonia solutions the indirect contributions to the potentials are strong functions of the temperature of the electron gas, which leads to a temperature dependence of the dielectric function. It is very difficult to describe this effect analytically. Therefore, the temperature effect has been evaluated numerically. For details see [2].

In [1, 2] the Geldart-Vosko approach was employed for the local field function G(x). This approach resulted in very strong screening effects which had led to potentials which were not able to reproduce the density correctly. Therefore, we used in this investigation the Ishimaru local field function [8] leading to a modification of the indirect site-site potentials. In this approach

$$G(x) = A x^4 + B x^2 + C ag{12}$$

$$+\left[Ax^{4}+\left(B+\frac{8}{3}A\right)x^{2}-C\right]\left(\frac{4-x^{2}}{4x}\ln\left|\frac{2+x}{2-x}\right|\right)$$

with

$$B = \frac{9}{16} \gamma_0 r_s - \frac{3}{64} [1 - g(0)] - \frac{16}{15} A, \qquad (13)$$

$$C = -\frac{3}{4}\gamma_0 r_s + \frac{9}{16}[1 - g(0)] - \frac{16}{15}A, \qquad (14)$$

$$g(0) = \frac{1}{8} \left(\frac{Y}{J(Y)} \right)^2. \tag{15}$$

$$A = 0.029$$
, $Y = 4 \left(\frac{\lambda r_s}{\pi}\right)^{1/2} = 4 \sqrt{1/\pi k_F}$,

$$r_{\rm s} = \left(\frac{9\,\pi}{4}\right)^{1/3}/k_{\rm F},\tag{16}$$

where J(Y) is a modified Bessel function.

The new total and direct potentials for the ammoniaammonia as well as the lithium-ammonia interactions are depicted in Figure 1. The full lines show that the new ab initio calculations lead to deeper minima compared with the previous ones [1]. The screening affects the two different interactions now in a similar way. The minima of both direct potentials are reduced by about 10% by the indirect contributions. A more detailed picture results from the site-site potentials which are presented in Figure 2.

The direct contributions to the ammonia-ammonia potential have not been changed compared with the previous ones [1, 5]. The indirect contributions to the N-H interaction differ significantly. The reduced

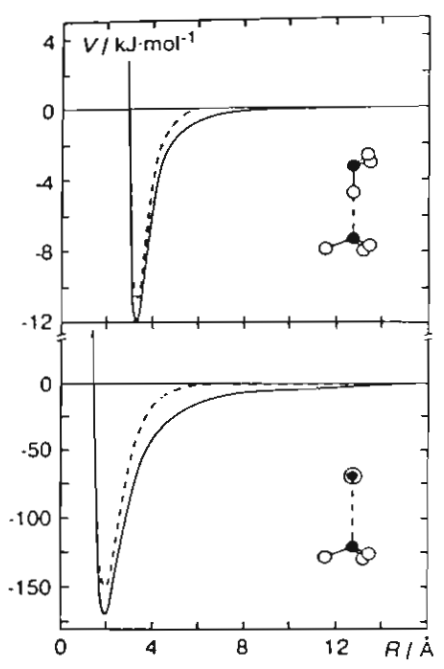


Fig. 1. Ammonia-ammonia (top) and lithium-ammonia (bottom) pair potentials as a function of nitrogen-nitrogen and lithium-nitrogen distances for orientations as shown in the insertion and at a temperature of 240 K with a lithium mole fraction of 0.1146. The full and dashed lines denote the direct and the total potential, respectively.

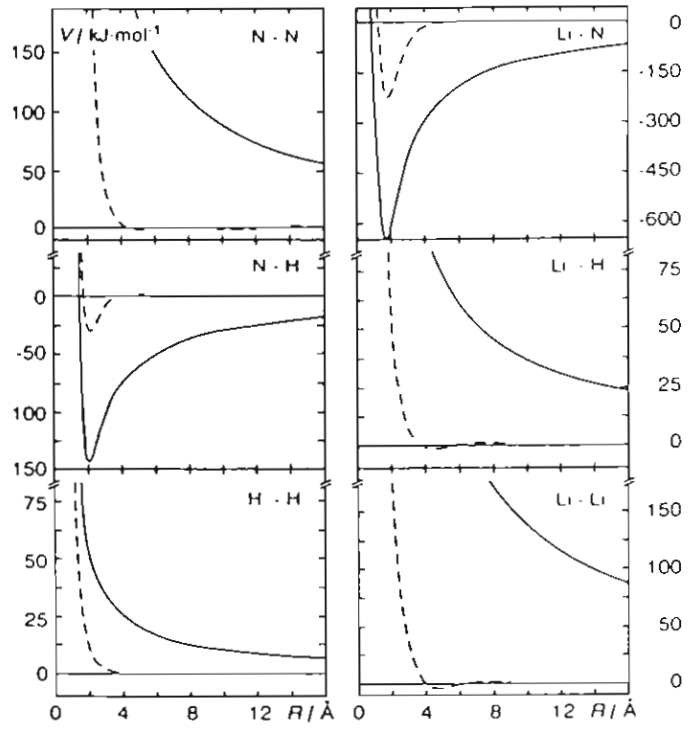


Fig. 2. Site-site potentials for the six different interactions in the lithium-liquid ammonia solution. The denotations are the same as in Figure 1.

The improved Li-N, Li-H and Li-Li direct contributions – resulting from the new ab initio calculations – differ significantly from the older ones [1, 5]. They are generally weaker. But the minimum in the lithium-ammonia potential is by about 20% deeper because of a smaller mutual compensation. With the modifications of the pseudopotential theory described above the screening becomes stronger in the case of the Li-N and Li-H interactions. Similar to the direct contributions, the mutual compensation of the site-site potentials leads again to a lower minimum in the total lithium-ammonia potential compared to the older one [1]. Differently, the screening of the Li-Li interactions is less pronounced and the minimum in the total Li-Li potential has become much shallower.

The Metropolis Monte Carlo method [9] was employed. The basic cube contained 135 lithium ions and 1025 ammonia molecules. With an experimental density of 0.554 g/cm³ at 240 K and 1 atm, a sidelength of the periodic cube of 37.89 Å resulted. Due to the strong screening of the Coulombic interactions by the indirect contributions (see Fig. 2). a cut-off of the total site-site potentials at 15 Å was justified, which saved a significant amount of computer time compared with the Ewald method. The starting configuration was randomly generated. The simulations were carried out for 40 million configurations in order to equilibrate the system. The next 3 million configurations were employed for the evaluation of the structural properties of the solution.

3. Results and Discussion

a) Radial Distribution Functions

The solvent-solvent, ion-solvent and ion-ion RDFs and the corresponding running integration numbers are presented in Figure 3. Their characteristic values as well as those obtained for a single lithium ion in 215 ammonia molecules [5] are summarized in Table 1. The coordination numbers are defined as the running integration numbers at the positions of the first minima of the RDFs.

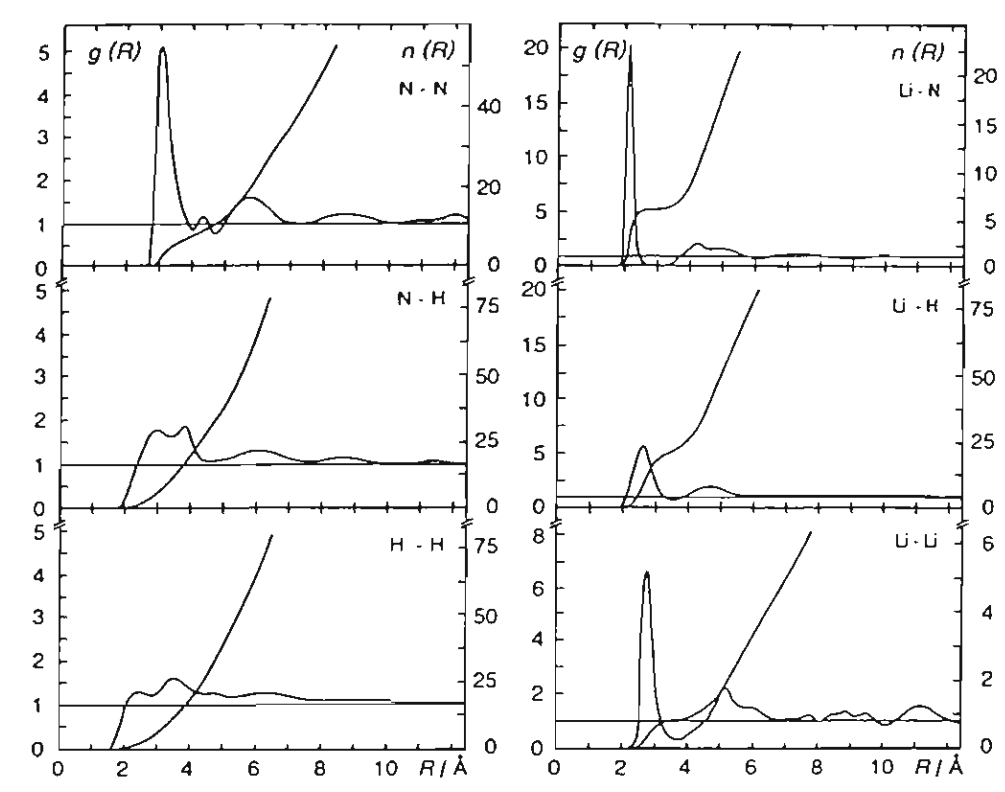


Fig. 3. Partial radial distribution functions and running integration numbers.

Table 1. Characteristic values of the radial distribution functions $g_{xy}(R)$. R_i , and R_{mi} are the distances in Å, where for the ith time $g_{xy}(R)$ is unity, has a maximum and minimum, respectively. The values for the dilute solution, $x_{Li} = 0.0046$, are also given for comparison.

xy	$x_{\rm Li} \cdot 100$	R_{i}	R_{M1}	$g_{xy}(R_{M1})$	R_2	$R_{m \iota}$	$g_{xy}(R_{m1})$	$R_{\rm M2}$	$g_{xy}(R_{M2})$	$n_{xy}(R_{m1})$
ии	11.98 0.46	2.80 3.04	3.04/4.32 3.38	5.1/1.2 2.2	3.88 4.29	4.06/4.68 5.0	0.9/0.7 0.7	5.92 6.64	1.6 1.2	8.1/10.7 12.8
НИ	11.98 0.46	2.40 3.11	3.00/3.82 3.62	1.8/1.9 1.3	- 4.47	4.48 4.9 – 5.3	1.1 0.8	6.00	1.4	28.6 34.2 – 43.4
нн	11.98 0.46	2.04 3.07	2.38/3.56 3.82	1.3/1.6 1.2	- 4.56	- 5.0 - 5.5	0.9	-	-	- 36.5-47.6
LiN	11.98 0.46	1.95 2.01	2.16 2.29	20.0 15.9	2.50 2.53	2.88 2.80	0.2 0.0	4.30 4.38	2.1 2.9	6.0 6.0
LiH	11.98 0.46	2.13 2.54	2.64 2.87	5.6 6.5	3.27 3.16	3.46 3.40	0.7 0.0	4.64 5.00	1.9 1.9	20.6 18.0
LiLi	11.98 0.46	2.51	2.74	6.6	3.25	3.72	0.3	5.24	2.3	0.8

Significant changes in the solvent structure can be observed by the comparison of the N-N, N-H and H-H RDFs for the two different concentrations. In the simulation with the single lithium ion, these RDFs are nearly the same as in pure ammonia [5]. The pseudopotential theory has not been employed in this case. Consequently, there exists no indirect contribution to the total potential.

The screening in the concentrated solution strongly reduces the repulsion for the N-N and H-H interactions (Fig. 2) and leads, therefore, to more pronounced first peaks in the corresponding RDFs at significantly shorter distances compared with the very dilute solution (Table 1). In spite of the fact that the potential minimum for the N-H interaction is also strongly reduced by the screening, the first peak in $g_{NN}(R)$ is more

pronounced. The reduction in the N-N and H-H repulsion overcompensates this effect, as can be seen from the total ammonia-ammonia potential depicted in Fig. 1, where the indirect contributions reduce the potential minimum by only about 10%.

In the concentrated solution, where 7.5 ammonia molecules are available for each lithium ion, the N-N RDF is in accordance with the formation of clusters where two solvated Li* have one, two or three ammonia molecules in common (see below). In such a cluster, where the six NH, molecules in the first solvation shell of lithium are octahedrally arranged (Table 1 and Fig. 4), one would expect about eight nearest neighbor nitrogen atoms around a central one at a distance of about 3 Å (first peak in $g_{NN}(R)$) and another two at about 4.3 Å, twice the Li-N distance (small intermediate peak) in agreement with the coordination numbers, $n_{NN}(R_{mi})$, given in the last column of Table 1. In keeping with this picture, both the first maximum and the first minimum in pure ammonia are found at distances longer by about 0.3 Å [5], resulting in a coordination number larger by about three than in the concentrated solution. Roughly speaking, the two Li + in the cluster are replaced by two ammonia molecules, and additional contributions come from the ammonia molecules in the bulk phase.

In accordance with the cluster formation, the second nearest ammonia neighbors would appear at about 6 Å (second peak in $g_{NN}(R)$; 0.7 Å shorter than in the dilute solution). This maximum is formed by the more than 30% ammonia molecules outside of the first solvation shells of the lithium ions.

The cluster formation in the concentrated solution leads – similar to $g_{NN}(R)$ – also in $g_{NH}(R)$ and $g_{HH}(R)$

to more pronounced first peaks at shorter distances than in pure ammonia [5]. The broad maxima there are splitted now. But it seems to be quite difficult to assign definite structures to the characteristics of these RDFs. Also the long range parts of all three solvent RDFs differ significantly for the two concentrations, which is again a consequence of the cluster formation.

The screening effect of the electrons leads to a slightly shorter distance of the first peaks in $g_{\rm LiN}(R)$ and $g_{\rm LiH}(R)$ when compared with the very dilute solution (Table 1). Although the coordination number does not change, the first peak in $g_{\rm LiN}(R)$ is slightly higher and that in $g_{\rm LiH}(R)$ slightly lower in the concentrated solution. Both first minima are less pronounced. The larger coordination number for hydrogen, $n_{\rm LiH}(R)$, is expected to result either from a less strong orientation of the solvation shell ammonia molecules because of screening effects, or from the undefined orientations of the ammonia molecules common to two lithium ions (see Figure 5).

The small effect of the lithium concentration on the structure of the solvation shell is in accordance with the only 10% decrease in the potential minimum of the lithium-ammonia interaction by the indirect contributions (Figure 1). The rather rigid solvation shell structure is confirmed by the finding that in 90% of all cases the coordination number is six while in only 5% each it is 5 or 7 (see also Figure 4).

The first peak in $g_{LiLi}(R)$ is quite pronounced at 2.4 Å. This distance is much shorter than the flat potential minimum between 4 and 5 Å (Figure 2). The running integration number is one at about 4.5 Å. This leads – as in $g_{NN}(R)$ – again to the conclusion that cluster formation must occur in spite of the fact that

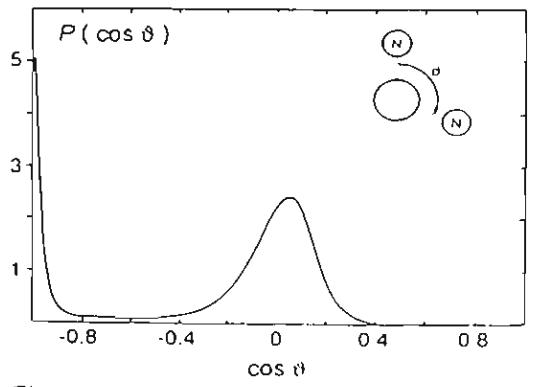


Fig. 4. Distribution of cos 9 - where 9 is defined as the nitrogen-lithium-nitrogen angle—calculated for the ammonia molecules in the first solvation shell of the lithium ion

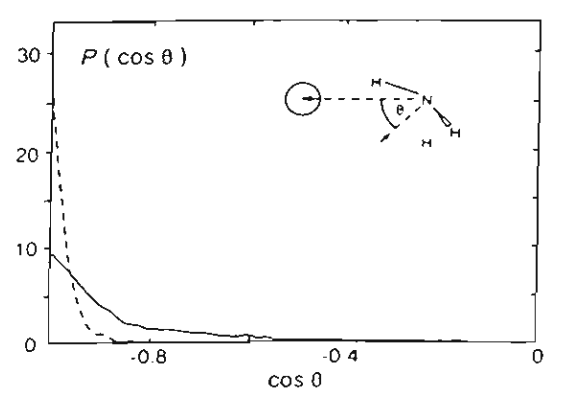


Fig. 5. Normalized distributions of $\cos\theta$ for the ammonia molecules in the first solvation shells of the lithium ions. θ is defined in the insertion. Full and dashed lines refer to lithium mole fractions of 0.1164 and 0.0046, respectively

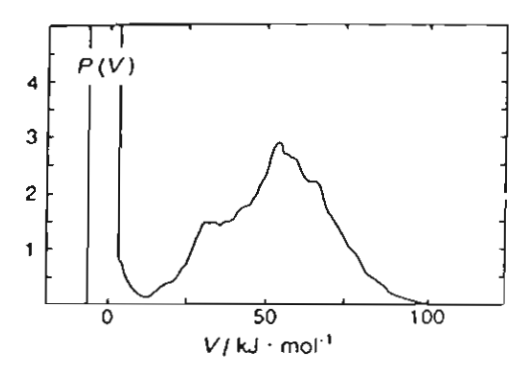


Fig. 6. Lithium-lithium pair interaction energy distribution in arbitrary units.

at least 30% of all ammonia molecules do not belong to a first solvation shell (see below).

The $g_{\text{LiLi}}(R)$ is in accordance with the pair interaction energy distribution, $P(V_{ij})$, shown in Figure 6. The positive energies at about 50 kJ/mol result from the interaction of two Li⁺ characterized by the first peak in $g_{\text{LiLi}}(R)$, as can be seen from a comparison with $V_{\text{LiLi}}^{\text{tot}}(R)$ depicted in Figure 2. The negative energies mainly result from those Li⁺ which belong to the second peak. At this distance $V_{\text{LiLi}}^{\text{tot}}(R)$ has its flat minimum. The large number of small positive interactions result from Li⁺ at distances larger than 6 Å.

b) Solvation Shell Structure

The geometrical arrangement of the ammonia molecules in the solvation shells of the lithium ions can be deduced from the simulation by the calculation of the distribution of cos 3, where 3 is defined as the N-Li-N angle. The result is depicted in Fig. 4, where only the ammonia molecules in the first solvation shells are included in the distribution.

It is obvious from Fig. 4 that the six ammonia molecules are arranged octahedrally around the lithium ion. The integration over the distribution shows that there is one other solvation shell molecule at about 180 and four more at about 90°. It is interesting to note that the maximum is not exactly at $\cos \theta = 0$ but shifted slightly to positive values, appearing at 86°. This slight disturbance of the octahedral arrangement might be caused by the cluster formation as discussed below, where one, two or three ammonia molecules belong simultaneously to the solvation shell of two tithium ions

c) Orientation of the Ammonia Molecules

The orientation of the ammonia molecules in the solvation shells of the lithium ions is described by the distribution of $\cos \theta$, where θ is defined as the angle between the dipole moment direction of the ammonia molecule and the vector pointing from the nitrogen atom towards the ion. The normalized distributions are presented in Fig. 5 for the two concentrations with the mole fractions 0.1164 (full) and 0.0046 (dashed).

For both concentrations there is a strong preference for the dipole moment of the ammonia molecule pointing away from the ion. The distribution is much broader for the concentrated solution. The reason for the significant difference in the widths of the distributions is expected to be connected with the cluster formation (see below). In the case of the single ion (dashed), solely the interaction between solvation shell molecule and the ion determines the orientation because of the relatively weak interactions between the solvation shell molecules and those in the bulk. In the concentrated solution, however, where - because of the cluster formation - one, two or three ammonia molecules belong simultaneously to the solvation shells of two lithium ions, there is a competition between the two ions for the energetically most favorable orientation leading to the broad distribution.

d) Cluster Formation

In order to understand in more detail the different features of the various RDFs depicted in Fig. 3, we have investigated in a first step the distribution of the ammonia molecules between the first solvation shells of the lithium ions and the bulk. An ammonia molecule is considered to belong to the first solvation shell if the Li-N distance is smaller than $R_{mi} = 2.88 \text{ Å}$, the position of the first minimum in the Li-N RDF. The coordination number of an Li^{*}, defined by $n_{\text{LiN}}(R_{\text{mi}})$, is found to be six (Table 1). It has been calculated from the simulation that 33% of all NH3 belong to the bulk. From the remaining 67% of the molecules, 55% are coordinated to one Li* and 12% simultaneously to two Li7. In the following discussion we shall denote these three kinds of NH3 molecules by NO, N1, and N2, respectively. It has been mentioned above that the formation of clusters explains the positions of the first as well as that of the small second peak in the N-N RDF. The shoulde: at the long distance side of the first peak results from the N-N distances in the bulk, where

a broad first maximum exists which is centered at 3.4 Å (Table 1).

The next point of interest is the distribution of the ammonia molecules N1 and N2 in the first solvation shells of the 135 lithium ions in the solution. With the denotation $Li(N1)_m(N2)_{6-m}$, the result is given in Table 2.

Table 2. The fraction in % of the clusters of kind m.

m	6	5	4	3	2
%	32	8	16	38	6

The structure of the clusters can be visualized easily. The octahedrally arranged solvation shells of two lithium ions have an NH3 molecule, an edge and a plane in common for m equal to 5, 4, and 3, respectively. For m2 one can imagine that a central solvated Li+ has two of his edges in common with two neighboring ones. From the numbers in Table 2 it could not be excluded that clusters with more than 3 Li+ exist in the solution as e.g. the cluster m2 could be imagined with five Li+ where four of them are combined with a central one by having one NH, molecule each in common. It will be demonstrated in the next paragraph that the probability to find such clusters is very small.

The number of nearest neighbor lithium ions around a central one up to the first minimum of the Li-Li RDF at 3.72 Å, $n_{LILI}(r_{mi})$, is 0.8, in accordance with the distribution given in Table 3.

- [1] Z. Gurskii, S. Hannongbua, and K. Heinzinger, Mol.
- Phys. 78, 461 (1993).
 Z. Gurskii, V. Kushaba, S. Hannongbua, and K. Heinzinger, Metal Phys. Adv. Techn. 17, 62 (1995).
 W. S. Benedict and E. K. Plyler, Can. J. Phys. 35, 890
- (1985).
- 4] F. H. Stillinger, Israel J. Chem. 14, 130 (1975).
- [5] S. Hannongbua, T. Ishida, E. Spohr, and K. Heinzinger, Z. Naturforsch. 43a, 572 (1988).

Table 3. Percentage of nearest neighbor lithium ions, n_{LiL} (R_{ml}) , around a central one.

n _{LILI} (R _{m1})	0	1	2	3	
%	40	44	14	2	

The Li-Li distances for the clusters m3, m4 and m5 are about 2.8, 3.1 and 4.3 Å, respectively. This means that clusters m5 and m6 do not contribute to the first peak in the Li-Li RDF and consequently $n_{LiLi}(R_{mi})$ =0, in agreement with Table 2. As there is no peak around 4.3 Å in $g_{LiLi}(R)$ and a shoulder can hardly be recognized, it has to be concluded that the number of clusters m5 is quite small, again in accordance with Table 2. This means also that in the clusters m4, m3 and m2 those with common edges and common octahedral planes are the by far most important ones, excluding contributions to these clusters from m5. The second peak in the Li-Li RDF must consequently almost exclusively result from the independently solvated lithium ions (m6).

Sarkar et al. [10] have deduced recently from a renewed evaluation of older X-ray data by Narten that clusters are formed in pure liquid ammonia at 277 K. This result cannot be related to the cluster formation here.

Acknowledgements

Financial support by the National Research Council of Thailand, the Thailand Research Fund, the Ukrainian Academy of Sciences and Deutsche Forschungsgemeinschaft is gratefully acknowledged.

- [6] T. H. Dunning, J. Chem. Phys. 53, 2823 (1970).[7] M. Dupuis, J. D. Watts, H. O. Villar, and C. T. Hurst, HONDO version 7.0 (1987), Documentation KGN (IBM Kingston 1988).
- S. Ishimaru and K. Utsumi, Phys. Rev. B24, 7385 (1981).
- [9] N. Metropolis, A. W. Rosenbluth, M. N. Rosenbluth, A. H. Teller, and E. Teller, J. Chem. Phys. 21, 1087 (1953).
- [10] S. Sarkar, A. K. Karmakar, and R. N. Joarder, J. Phys. Chem. A101, 3702 (1997).

CHEMICAL PHYSICS LETTERS

Chemical Physics Letters 288 (1998) 663-668

On the solvation of lithium ions in liquid ammonia: Monte Carlo simulations with a three-body potential

Supot Hannongbua

Chemistry Department, Faculty of Science, Chulalongkorn University, Bangkok 10330, Thailand

Received 6 January 1997; in final form 23 March 1998



EDITORS: A D. BUCT LAM, D.A. KING, A H. ZEWAIL Assistant Editor Cambridge, UK

FOUNDING EDITORS: G.J. HONTINK, E. JANSEN. FORMER EDITORS: R.B. BERNSTEIN, D.A. SHIRLEY, R.N. ZARF

ADVISORY EDITORIAL BOARD

Australia

B.J. ORR. Sydney

F.C. DE SCHRIJVER, Heverlee (Leuven)

P.A. HACKETT, Oitawa J.W. HEPBURN, Waterloo CA McDOWELL, Vancouver

F RESENBACHER, Aarhus G.D. BILLING, Copenhagen

Frai

E. CL_1ENTI, Strasbourg J. DURUP, Toulouse J.-M. LEHN, Strasbourg B. SOEP, Orsay

Germany

R. AHLRICHS, Karlsruhe V.E. BONDYBEY, Garching W. DOMCKE, Dusseldorf G. ERTL, Berlin G.L. HOFACKER, Garching W. KIEFER, Würzburg D.M. KOLB (Jm. J. MANZ. Berlin M. PARRINELLO, Shittgart S.D. PEYERIMHOFF, Bonn R. SCHINKE, Göttingen EW. SCHLAG, Garching J. TROE, Gottingen H.C. WOLF, Stuttgart

India

C.N.R. RAO, Bangalore

W. ZINTH, Munich

J. JORTNER, Tel Aviv R.D. LEVINE, Jerusalem traly

V. AQUILANTI, Perugia

Japan

H. HAMAGUCHI, Tokyo M. ITO. Okazaki T. KOBAYASHI, Tokyo K. KUCHITSU, Sakado H NAKATSIJI KVOIO K. TANAKA, Tokyo K. YOSHIHARA, Tar. Jauchi

People's Reposite of China C.-H. ZHANG, Beijing

Poland

Z.R. GRABOWSKI, Warsaw

Russian Federation

A.L. BUCHACHENKO, Moscow V.S. LETOKHOV, Troitzk Yu.N. MOLIN, Novosibirsk

Spain

A. GONZÁLEZ UREÑA, Madrid

Sweden

B.O. ROOS, Lund V. SUNDSTRÖM, Lund

Switzerland

M. CHERGUL Lausanne-Dorigny

R.R. ERNST, Zurich M. QUACK, Zurich

Taiwan, ROC

Y.T. LEE, Taipei The Netherlands

AJ. HOFF, Leiden A.W. KLEYN, Amsterdam R. VAN GRONDELLE, Amsterdam D.A. WIERSMA, Groningen

United Kingdom M.N.R. ASHFOLD, Bristol G.S. BEDDARD, Leeds D.C. CLARY, London R. FREEMAN, Cambridge R H. FRIEND, Cambridge

N.C. HANDY, Cambridge A C LEGON, Evr. of R.M. LYNDE + BULL, Belfast

JP C' J. Oxford . SMITH, Birnungham

P.F. BARBARA, Minneapolis, MN E.A. CARTER, Los Angeles, CA

A.W. CASTLEMAN Jr., University Park, PA

S.T. CEYER, Cambridge, MA D. CHANDLER, Betkeley, CA F.F. CRIM, Madison, WI

A DALGARNO, Cambridge, MA C.E. DYKSTRA, Indianapolis, IN K B EISENTHAL, New York, NY

M.A. EL-SAYED, Atlanta, GA M.D. FAYER, Stanford, CA G.R. FLEMING, Berkeley, CA

R M HOCHSTRASSER, Philadelphia, PA S.R. LEONE, Boulder, CO

M.I. LESTER, Philadephia, PA W.C. LINEBERGER, Boulder, CO. B.V. McKOY, Pasadena, CA W.H. MILLER, Berkeley, CA W.E. MOERNER, La Jolla, CA K. MOROKUMA, Atlanta, GA S. MUKAMEL, Rochester, NY D.M. NEUMARK, Berkeley, CA

A. PINES, Berkeley, CA

A F. RAVISHANKARA, Boulder, CO S A. RICE, Chicago, IL PJ. ROSSKY, Austin, TX RJ SAYKALLY, Berkeley, CA H F SCHAEFER III, Athens, GA GC SCHATZ, Evansion, IL R E SMALLEY, Houston, TX G.A. SOMORJAI, Berkeley, CA W.C. STWALLEY, Storrs, CT

D.G. TRUHLAR, Minneapolis, MN G.M. WHITESIDES, Cambridge, MA C WITTIG, Los Angeles, CA P.G. WOLYNES, Urbana, IL JT YATES Jr., Pattsburgh, PA R.N. ZARE, Stanford, CA

Contributions should, preferably, be sent to a member of the Advisory Editorial Board (addresses are given in the first issue of each volume) who is familiar with the research reported, or to one of the Editors:

> A.D. BUCKINGHAM D.A. KING Editor of Chemical Physics Letters University Chemical Laboratory Lensfield Road Cambridge CB2 1EW, UK FAX 44-1223-336362

A.H. ZEWAIL Editor of Chemical Physics Letters A.A. Noyes Laboratory of Chemical Physics California Institute of Technology Mail Code 127-72 Pasadena, CA 91125, USA FAX 1-626-4050454

After acceptance of the paper for publication, all further correspondence should be sent to the publishers (Mr. M.J.A. Jarmuszewski, Issue Management, Elsevier Science B.V., P.O. Box 2759, 1000 CT Amsterdam, The Netherlands; Tel.: (31-20) 485-3434; Fax: (31-20) 485-2775 e-mail m jarmuszewski/5/elsevier.nl)

Publication information: Chemical Physics Letters (ISSN 0009-2614). For 1998, volumes 281-297 are scheduled for publication. Subscription prices are available and the scheduled for publication. able upon request from the publisher. Subscriptions are accepted on a prepaid basis only and are entered on a calendar year basis. Issues are sent by surface mail except to the following countries where Air delivery via SAL is ensured: Argentina, Australia, Brazil, Canada, Hong Kong, India, Israel, Japan, Malaysia, Mexico, New Zealand, Pakistan, PR China, Singapore, South Africa, South Korea, Taiwan, Thailand, USA. For all other countries airmail rates are available upon request. Claims for missing issues must be made within six months of our publication (mailing) date

Copyright © 1998, Elsevier Science B V. All rights reserved

0009-2614-1998/\$19-09

C

01

m

ef

lic

3.1

F113

US mailing notice - Chemical Physics Letters (ISSN 0009-2614) is published weekly by Elsevier Science B.V., Molenwerf 1, P.O. Box 211, 10(s) AE Amsterdam Annual subscription race in the USA US\$ 8(04) 00, including air speed delivery valid in North, Central and South America only Periodicals postage paid at Jamaica, NY 11431. USA POSTMASTERS. Send address changes to Chemical Physics Letters. Publications Expediting, Inc., 218) Meacham Avenue, Elmoni, NY 11003. Airfreight and mailing in the USA by Publication Expediting.



CHEMICAL PHYSICS LETTERS

Chemical Physics Letters 288 (1998) 663-668

On the solvation of lithium ions in liquid ammonia: Monte Carlo simulations with a three-body potential

Supot Hannongbua

Chemistry Department, Faculty of Science, Chalalongkorn University, Bangkok 10330, Thailand

Received 6 January 1997, in final form 23 March 1998

Abstract

Many-body effects in the Li^*-NH_3 system have been examined, using ab initio calculations. Potential energy surfaces of the three-body effect in the $Li^*-(NH_3)_2$ complex have been demonstrated. A three-body potential function was developed from more than 6000 configurations of the $Li^*-(NH_3)_2$ complexes. Monte Carlo simulations were performed with and without the three-body correction functions. The results show that the error of the pair approximation in the octahedral complex is 23%. Only slight changes in the three-body energies due to rotation of the molecules in the tetrahedral and octahedral complexes were yielded and they were excluded from the development of the three-body correction function. The first shell coordination number of 6 is the same for both simulations. © 1998 Elsevier Science B.V. All rights reserved.

1. Introduction

It has been found that the assumption of pairwise additivity leads to an error of interaction energies in cation—water systems of at least 10%, 15% and 20% for mono-, di- and trivalent ions, respectively [1]. In metal—ammonia systems, energetic errors due to many-body effects for $M(NH_1)_n$ clusters, where M is Na⁺, Be²⁺, Mg²⁺, Zn²⁺ and Al³⁺ and n=1+8, have been investigated {2.3}, yielding errors in the two-body approximation in the octahedral complexes of 17%, 43%, 30%, 18% and 43%, respectively. By means of Monte Carlo simulations [2,4], three-body effects reduce the first shell coordination number liquid ammonia from 9 to 8 for Na⁺, 10 to 6 for Mg²⁺ and 9 to 8 for Zn²

For Li⁺, apart from the composition Li(NH₃)₄⁺ of highly concentrated solutions in frozen form (see, e.g., Refs. [5,6]), a precise stoichiometry of the first solvation shell of Li⁺ in NH₃ is, surprisingly, not yet known. The only available information for dilute solutions is from molecular dynamics simulations by us [7] and Impey and Klein [8], leading to first-shell coordination numbers of 6 and 4, respectively. In addition, an octahedral complex Li(NH₃)₆⁺ has also been found in by—concentration ranges [9].

In continuation of our previous work on dilute solutions of metal ions in liquid ammonia [24,7,10,11] and on concentrated lithium-ammonia solutions [9,12,13], we have extended the Monte Carlo simulation of the dilute lithium-ammonia solution to a level including three-body corrections.

(MR9)-2614/98/\$19 (M) (=1998 F) = - whence B V All rights reserved PH | \$10009 (2614 (98)09).

with

set ier

availe mail aysia, iilable

319.00

XI AE xdicals acham

26532

The goal of this study was to investigate the relative importance of the three-body effects on angural properties of the solution.

2. Details of the calculations

2.1. Many-boxy effects and three-body correction functions

To examine energetic errors due to many-body effects in the Li*-NH, system, ab initio calculations in a double-zeta basis set including polarization functions (DZP) [14] have been performed using the Gaussian 92 program [15] for the Li(NH,), complex. The N-Li* distances have been simultaneously optimized. The experimental gas phase geometry of the ammonia molecule, with an N-H distance of 1.0124 Å and an HNH angle of 106.7°, was taken from the literature [16] and kept constant throughout. The average binding energy per ammonia molecule is computed as

$$\Delta E_{av} = \left[E(ML_6) - E(M) - E(L_6) \right] / 6$$
. (1) where $E(ML_6)$, $E(M)$ and $E(L_6)$ are the total energies of the Li(NH₃)₆ complex, the Li and six NH₄ molecules in the same configuration as that of Li(NH₃)₆, respectively. This yields an error in the pair approximation of 23%.

In order to develop the complete three-body function, a second ammonia molecule was placed at ierous positions around the first-ammonia/Li complex (Fig. 1), varying the geometrical parameters $0^{\circ} \le \Theta \le 180^{\circ}$, $0^{\circ} \le \phi \le 60^{\circ}$ and $1.5 \text{ Å} \le r_2 \le 8.0 \text{ Å}$. The Li '-NI distance (r_3) of 1.5 Å and the configuration of the first ammonia were at first kept fixed and the calculations were performed for numerous Li '-(NII₃)₂ clusters. Then the same procedure was repeated for $r_1 = 1.8$, 2.02, 2.2, 2.5, 3.0, 4.0, 6.0 and 8.0 Å, leading to a total of more than 6000 configurations of Li '-(NH₃)₂ complexes and 18000 Li '-NH₃ and NH₃-NH₃ pair interactions.

The three-body interaction energies were calculated as:

$$\Delta E_{\text{Mod}} = \left\{ E[ML_1L_2] - E[M] - E[L_1] - E[L_2] \right\} - \left\{ E[L_1L_2] - E[L_1] - E[L_2] \right\} - \sum_{i=1}^{2} \left\{ E[ML_i] - E[M] - E[L_i] \right\}.$$
 (2)

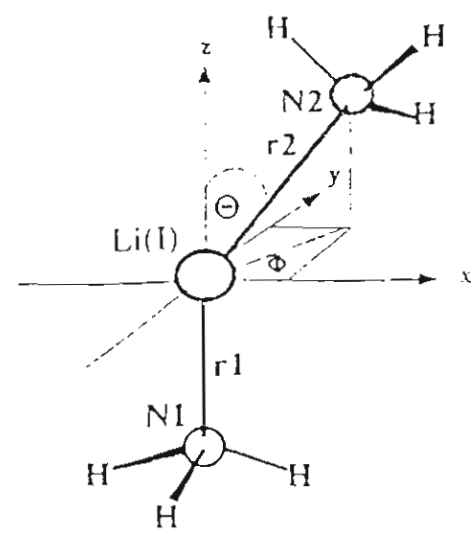


Fig. 1. Geometrical parameter definitions in the evaluation of the Li^+ -(NH $_1$)₂ potentials, used for the SCF calculations.

All energies on the right-hand side of Eq. (2) are the total energies of the system in brackets, where M, L₁ and L₂ denote the lithium ion and the first and second ammonia molecules, respectively. Then these energies were fitted to an analytical potential of the following type:

$$\Delta E_{\text{thd}} = a e^{-b(r_1 + r_2)} e^{-r_1}.$$
 (3)

Here a, b and c are fitting parameters, r_3 is the distance between N1 and N2 of the two ammonia molecules, and r_1 and r_2 are the distances from Li to N1 and N2, respectively. The final fitting parameters for the three-body functions according to Eq. (3) are the following: a = 156.783 kcal mol⁻¹, $b = 0.2261 \text{ Å}^{-1}$ and $c = 0.9645 \text{ Å}^{-1}$.

2.2. Monte Carlo simulations

Monte Carlo simulations have been performed for a system consisting of one Li⁺ and 201 ammonia molecules, using our previous Li⁺-NH₃ and NH₃-NH₃ potentials [7,9], with and without the three-body correction functions. The experimental density of pure liquid ammonia at 277 K and 1 atm of 0.690 g cm⁻¹ leads to a basic box length of 20.99 Å. A starting configuration was generated randomly and a further 5 million configurations after equilibration were used to evaluate structural data of the solution.

3. Results and discussion

3.1. Characteristics of the three-body correction function

The nature of the three-body correction terms for the Li*-(NH₃)₂ complexes is similar to those observed by us [2,4] for $Zn^{2+}-(NH_1)_2$, $Na^+-(NH_3)_3$ and Mg2 -(NH₃), by Lybrand and Kollman [17] for Mg²⁺-(H₂O)₂ and by Ortega-Blanke et al. [18] for $Mg^{2+}-(H_2O)$, and $Ca^{2+}-(H_2O)$, where the interactions are attractive at short distances (< 1.8 Å) and repulsive for the other ranges. The variations of the term for Li⁺-(NH₃)₂, as a function of r_2 for different values of Θ (see Fig. 1), where $r_1 = 2.0 \,\text{Å}$ and $\phi = 0^{\circ}$, are displayed in Fig. 2. As in the other cases [4,17,18], the attractive SCF data points in the region of $r_1, r_2 < 1.8 \text{ Å}$ were not represented by the three-body functions because they were not included in the fit. This simplification was found not to affect the accuracy of the simulation results, since the repulsive terms of the pair potential dominate within this region. In Fig. 2, a good agreement between the calculated (ΔE_{SCF}) and plotted (ΔE_{FIT}) energies was yielded. Note that the fit is weighted to the configurations where the NI-Li*-N2 angles are ≥ 90°, as they are known to correspond to those of the tetrahedral or octahedral angles which are favored geometries of the ions in the solution.

To evaluate in more detail the angular dependence of the three-body function, a three-dimensional ΔE_{3bd}

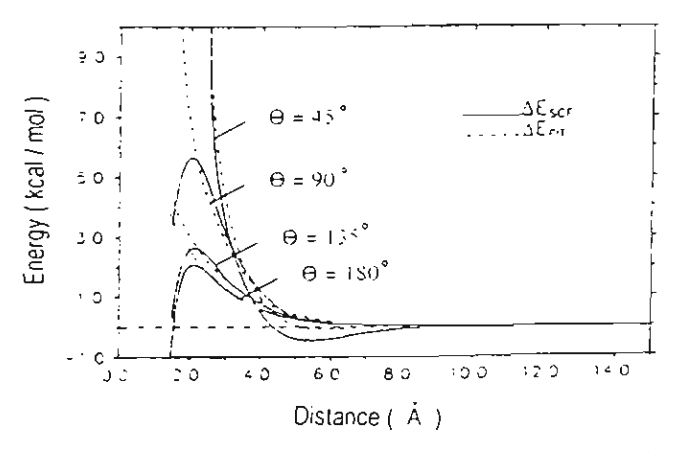


Fig. 2. Variation of the three-body energies obtained from the SCF calculations and from the fitted analytical potential, as a function of r_2 , where $r_3 = 2.02 \,\text{Å}$ and $\phi = 0$ for different coacs of G (see Fig. 1).

10 TO 1

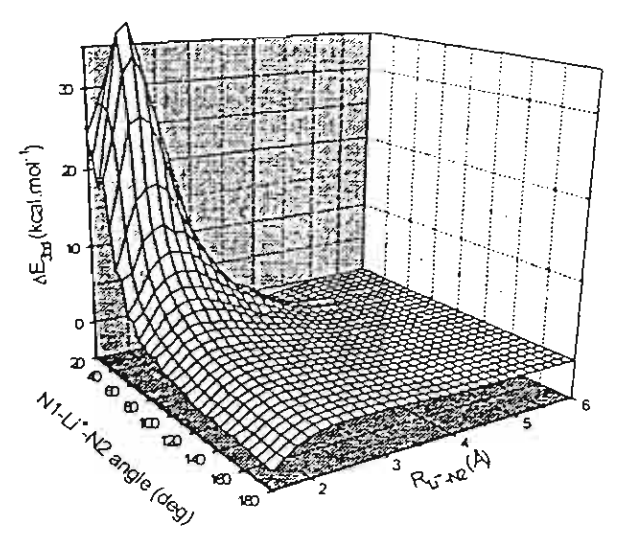


Fig. 3. Potential energy surfaces for the three-body effects in the Li^* - $(\mathrm{NH}_3)_2^*$ complex as a function of the NI - Li^* - $\mathrm{N2}$ angle and Li^* - $\mathrm{N2}$ distance, where the Li^* - $\mathrm{N1}$ distance is 2.02 Å and $\mathrm{N1}$ and $\mathrm{N2}$ denote nitrogen atoms of the first and the second ammonia molecules, respectively (see text for more details).

plot was generated. The Li⁺ is placed at the origin of the coordinate system and the nitrogen atom of the first ammonia molecule (N1) is fixed in the positive x-axis at an Li⁺-N1 distance $(r_1) = 2.02 \,\text{Å}$ (distance where the minimum of the Li⁺-NH₃ pair potential takes place, r_{op}), pointing with its dipole moment vector toward Li⁺. One of its hydrogen atoms lies in the xz-plane. The nitrogen atom of the second ammonia molecule (N2) is moved along with radius $r_2 = 1.5 \,\text{Å}$ and $30^\circ \le \alpha \le 180^\circ$, where α denotes the N1-Li⁺-N2 angle, also with its dipole vector pointing to the ion and one of its hydrogens in the xz-plane. The same procedure was repeated for $r_2 = 1.8, 2.02, 2.2, 2.5, 3.0, 4.0$ and $6.0 \,\text{Å}$. The resulting ΔE_{3bd} plot is displayed in Fig. 3.

It is clearly seen from the plot that at short r_1 and r_2 distances, ΔE_{3bd} depends strongly on the N1-Li⁺-N2 angle. Decreasing the angle leads to an exponential increase in the energy. The ΔE_{3bd} values at r_{op} and the N1-Li⁺-N2 angles of 90, 104.5 and 180°, which correspond to those of tetrahedral and octahedral r_{op} argurations, are 3.6, 2.3 and r_{op} 0.1 keal mot in espectively. Including a thermal effect at r_{op} 1 of 0.6 keal mot in the minimum N1-Li⁺-N2 angle which should take place in the solution is r_{op} 1. Although the ΔE_{3bd} 1 at small N1-Li⁺-N2 angles and short N-Li⁺ distances is relatively high

(Fig. 3), such configurations are rarely detected during simulations due to the strong repulsion of the pair potential. In addition, as a function of the Li^+ -N distance, $\Delta E_{\rm ind}$ for any N1-Li⁺-N2 angle shows a maximum at $r_{\rm so}$.

Investigations have also been undertaken to examine the effect of the rotation of the ammonia motecules on ΔE_{Abd} . Here, r_1 and r_2 were fixed at $r_{\rm ep}$, for values of the N1-Li⁺-N2 angle between 30 and 180°, while the second ammonia molecule was (tated around its dipole vector. The rotation step was 10°, ranging from 0 to 90°. The results of the calculations are depicted in Fig. 4. Rotation of the second ammonia molecule in the Li^* -(NH₃), complex has a strong effect on the changes in ΔE_{38d} only for small N1-Li*-N2 angles and hence for short N1-N2 distances. It is interesting to note that the rotation of the molecules around their dipole axes in the tetrahedral and octahedral clusters causes only slight changes in the three-body energies. The maximal fluctuations of ΔE_{3bd} under molecular rotation for any N1-Li*-N2 angles between 90 and 180°. i.e. 0.5 kcal mol⁻¹, is even less than thermal fluctuations at 298 K. The result clearly indicates that rotation of the molecule can be excluded from the

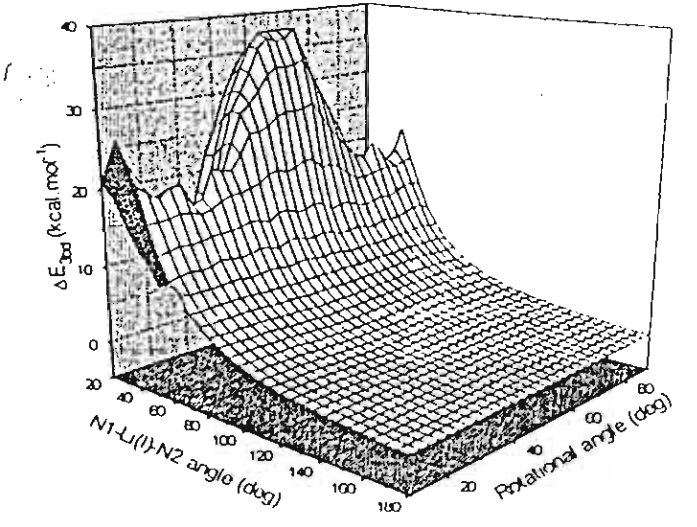


Fig. 4. Potential energy surfaces for the three-body effects in the L(r') (NH $_3$)₂ complex as a function of the N1+L $_4$ ' - N2 angle and angle of rotation of an aminonia molecule, where L(r') N1 and L(r') N2 distances are $2.02\,\tilde{\Lambda}$ and N1 and N2 denote introgen atoms of the first and the second aminonia molecules, respectively (see text for more details).

development of the three-body correction function. This reduces the computational time required for the quantum chemical calculations. In addition, neglect of this phenomenon in our Li^* -(NH₃)₂ functions (Eq. (3)) is also the consequence of this finding.

4. Monte Carlo simulations

As expected and found in our previous work [2,4], no significant difference between the atom-atom radial distribution functions (RDFs) of the ammonia molecules for both simulations, with and without three-body corrections, is detected, as far as position and height of the peaks and coordination numbers are concerned. The results are in good agreement with X-ray [17] and other simulation data [7,8,18–23].

The Li'-N and Li'-H RDFs obtained from the simulations with and without the three-body correction functions are shown in Fig. 5. Corresponding plots for Na taken from the literature [4] are also given for comparison. For all RDF plots, the difference in the position of the peaks for both runs is almost negligible. The first solvation sphere of the Lt' is represented by a sharp peak centered at 2.20 A. The corresponding coordination numbers (integrated up to the first minima of the two Li*-N RDFs) of 6 are identical. Influence of the three-body corrections leads to a slightly decreased probability of finding a solvent molecule in the region between the first and second solvation shells, and hence a slight lowering of the first minima of the Li*-N and Li' H RDFs. To keep a constant first shell coordination number, compensation was apparently achieved by a slight increase in the first peaks (Fig.

Some comments could be made concerning the influence of the three-body correction on the first shell coordination number of Li⁺, especially in comparison with that of Na⁺. Although the energetic error of the pair approximation in the octahedral complex for the Na⁺ of 18% is lower than that of 2.3% for Li⁺, the three-body correction reduces the first shell coordination number of Na⁺ in liquid ammonta from 9 to 8 [4]. This is a consequence of the size of the ions. The smaller ion Li⁺ can move

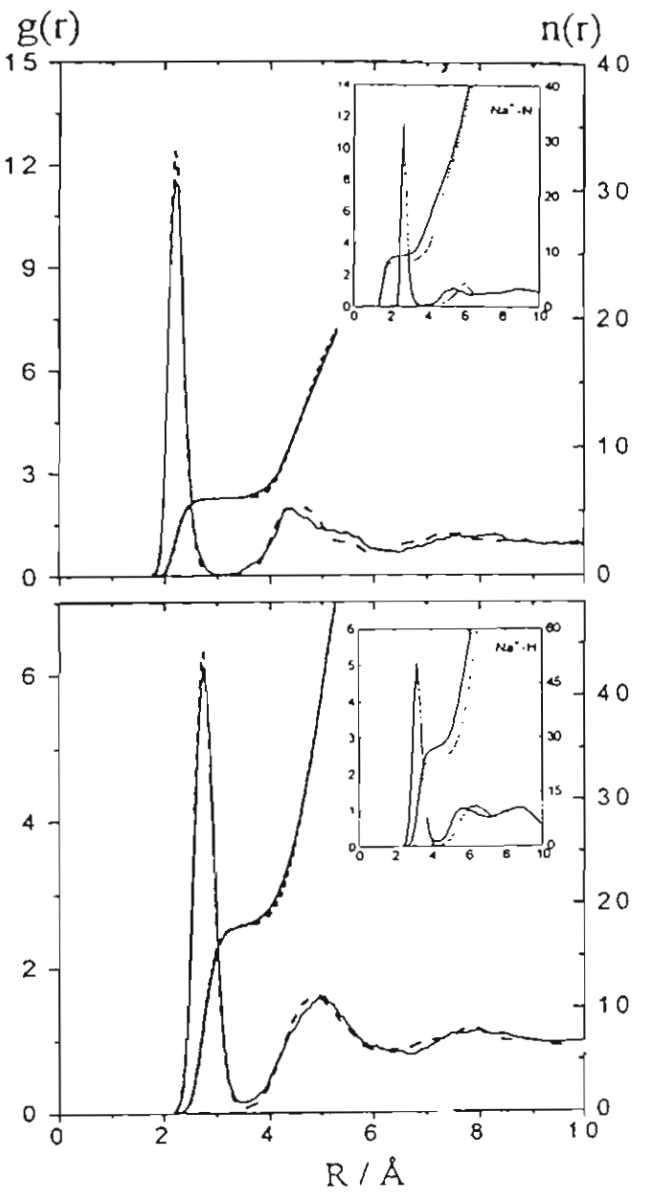


Fig. 5. Li^{*}~N (above) and Li^{*}-H (below) radial distribution functions and corresponding running coordination numbers in a dilute lithium-ammonia solution, obtained from the simulations without (solid line) and with (dashed line) three-body corrections. The same plots for Na^{*} are shown (insets) for comparison.

only by carrying some of the solvent molecules with it, thus rendering it more effective than the large ion, which is only loosely bound to the solvent.

The calculated average coordination number of 6 conflicts with that of 4 inferred by Impey and Klein [8], based on a molecular dynamics study of a solution of one Li in 107 NH, molecules. However,

this simulation was performed using a modified Li⁺-H₂O potential, which is less negative than our SCF Li⁺-NH₃ pair-potential. The Li⁺-NH₃ and the Li⁺-H₂O interaction energies, computed with the DZP basis set [14] at the optimal configuration of the Li⁺-NH₃ complex (the Li⁺-N distance is 2.02 Å) have been examined. The corresponding energies are –40.6 and –36.2 kcal mol⁻¹, respectively. Therefore, it is clear that the source of the lower coordination number reported by Impey and Klein lies in the less negative modified Li⁺-H₂O potential for association of the ion to the solvent molecule.

As experimental data on the structural properties of Li+-NH, solution are available only for the crystalline phase or in frozen form (see, e.g., Refs. [5,6,19-23]) and theoretical approaches exist only for high Li⁺ concentration, where the solutions are characterized by excess electrons and the coordination number of Li is not taken into consideration [24-26], there is no way at present to ascertain whether the obtained solvation numbers are in better agreement with experiment when using three-body potentials than when using two-body potentials only. Although more extensive investigations have been made for metal ions in aqueous solution, much of the available data, which are comprehensively reviewed by Marcus [27] and taken from both experimental and theoretical methods, show inconsistencies between the values deduced from different sources. Based on computer simulation techniques including three-body corrections, it is particularly agreed that this approach, despite its shortcomings, shows ways in which generally available methods can be used to improve upon the model and hence the structural information of the solution [1,2,4,17,18]. Therefore, the inclusion of at least three-body effects seems to he absolutely necessary.

Acknowledgements

Financial support by the Thailand Research Fund and the generous supply of computer time by the Austrian-Thai Center for Computer Assisted Chemical Education and Research in Bangkok and the National Electronic and Computer Technology Center, Bangkok, Thailand, and the computing center of

Innsbruck University, Austria, and of Max-Planck-Institution of Chemie, Mainz, Germany, are gratefully mowledged. The author wishes to thank Dr. D. Ruffolo for proof-reading the manuscript and Dr. S. Kokpol, Dr. K. Heinzinger and Professor Z. Gurskii for helpful discussions and comments.

References

- M.M. Probst, Chem. Phys. Lett. 137 (1987) 229.
 S. Hannonghua, T. Kerdcharoen, B.M. Rode, J. Chem. Phys. 96 (1992) 6945.
- [3] T. Kerdcharoen, Hot-spot molecular dynamics, Ph.D. Thesis University of Innsbruck, Innsbruck (1995).
- [4] S. Hannonghua, J. Chem. Phys. 106 (1997) 6076.
- [5] R.W. Marzke, W.S. Glaunsinger, J. Phys. Chem. 79 (1975) 2976.
- [6] P. Chieux, H. Bertagnolli, J. Phys. Chem. 88 (1984) 3726.
- [7] S. Hannongbua, T. Ishida, E. Spohr, K. Heinzinger, Z. Naturforsch. 43a (1988) 572.
- [8] R.W. Impey. M.L. Klein, J. Chem. Phys. 83 (1985) 5802.
- [9] Z. Gurskii, S. Hannongbua, K. Heinzinger, Mol. Phys. 78 (1993) 461.
- [10] S. Hannongbua, Aust. J. Chem. 44 (1991) 447.
- [11] S. Hannongbua, B.M. Rode, Chem. Phys. 162 (1992) 257.
- [12] Z. Gurskii, V. Kushaha, S. Hannongbua, K. Heinzinger, J. Metals Phys. Adv. Tech. 17 (1995) 62.

- [13] S. Hannongbua, S. Kokpol, Z. Gurskii, K. Heinzinger, Z. Naturforsch, 52a (1997) 828.
- [14] T.H. Dunning, J. Chem. Phys. 53 (1970) 2823
- [15] M.J. Frisch, G.W. Trucks, M. Head-Green, and M. Gill, M.W. Wong, J.B. Foresman, B.G. Tobeson, H.B. Schlegel, M.A. Robb, E.S. Replogle, C. Lomperts, J.L. Andres, K. Raghavachari, J.S. Binther, G. Gonzalez, R.L. Martin, D.J. Fox, D.J. DeFree, A. Baker, J.J.P. Stewart, J.A. Pople Gaussian, 97 Nevision, A. Gaussian, Inc., Physburgh, PA, 1992.
- [16] W.S. Benedict, E.K. Plyler, Can. J. Phys. 35 (1985) 890.
- [17] T.P. Lybrand, P.A. Kollman, J. Chem. Phys. 88 (1985) 2923.
- [18] L. Ortega-Blanke, J. Hernandez, O. Novaro, J. Chem. Phys. 81 (1984) 1894.
- [19] F. Leclercq, P. Damay, P. Chieux, J. Phys. (Paris) IV (1991) C5-359.
- [20] V.G. Young, W.S. Glaunsinger, J. Am. Chem. Soc. 111 (1989) 9260.
- [21] W.S. Glaunsinger, J. Phys. Chem. 84 (1980) 1163
- [22] W.H. McKnight, J.C. Thompson, J. Phys. Chem. 79 (1975) 2984.
- [23] W.S. Glaunsinger, M.J. Sienko, J. Phys. Chem. 62 (1975) 1873.
- [24] J. Kohanoff, F. Budu, M. Parrinello, M.L. Klein, Phys. Rev. 73 (1994) 3133.
- [25] Z. Deng, G.J. Martyna, M.L. Klein, Phys. Rev. 71 (1993) 267.
- [26] G.J. Martyna, Z. Deng, M.L. Klein, J. Chem. Phys. 98 (1993) 555.
- [27] Y. Marcus, Chem. Rev. 88 (1988) 1475.

Orders, claims, and product enquiries: please contact the Customer Support Department at the Regional Sales Office nearest to you:

New York
Elsevier Science
P.O. Box 945
New York, NY 10159-0945
USA
Tel. (+1)212-633-3730
[Toll free number for North
American customers:
1-888-4ES-1NFO (437-4636)]
Fax (+1)212-633-3680
e-mail: usinfo-f@elsevier.com

Amsterdam
Elsevier Science
P.O. Box 211
1000 AE Amsterdam
The Netherlands
Tel. (+31)20-4853757
Fax (+31)20-4853432
e-mail: nlinfo-f@elsevier.nl

Tokyo
Elsevier Science
9-15 Higashi-Azabu 1-chome
Minato-ku, Tokyo 106
Japan
Tel. (+81)3-5561-5033
Fax (+81)3-5561-5047
e-mail. info@elsevier.co.jp

Singapore
Elsevier Science
No. I Temasek Avenue
#17-01 Millenia Tower
Singapore 0.39192
Tel. (+65)434-3727
Fax (+65)337-2230
e-mail: asiainfo@elsevier.com.sg

Advertising information: Advertising orders and enquiries may be sent to: International: Elsevier Science, Advertising Department, The Boulevard, Langford Lane, Kidlington, Oxford OX5 1GB, UK, Tel. (+44)(0)1865 843565, Fax (+44)(0)1865 843976. USA and Canada: Weston Media Associates, Daniel Lipner, P.O. Box 1110, Greens Farms, CT 06436-1110, USA, Tel. (+1)(203)261-2500, Fax (+1)(203)261-0101. Japan: Elsevier Science Japan, Marketing Services, 1-9-15 Higashi-Azabu, Minato-ku, Tokyo 106, Japan, Tel. (+81)3-5561-5033, Fax (+81)3-5561-5047.

Electronic manuscripts: Electronic manuscripts have the advantage that there is no need for the rekeying of text, thereby avoiding the possibility of introducing errors and resulting in reliable and fast publication.

Your disk plus three, final and exactly matching printed versions should be submitted together. Double density (DD) or high density (HD) diskettes $(3^{1/2} \text{ or } 5^{1/4} \text{ inch})$ are acceptable. It is important that the file saved is in the native format of the wordprocessor program used. Label the disk with the name of the computer and wordprocessing package used, your name, and the name of the file on the disk. Further information may be obtained from the Publisher.

Authors in Japan please note: Upon request, Elsevier Science Japan will provide authors with a list of people who can check and improve the English of their paper (before submission). Please contact our Tokyo office: Elsevier Science Japan, 1-9-15 Higashi-Azabu, Minato-ku, Tokyo 106; Tel. (03)-5561-5032; Fax (03)-5561-5045.

Chemical Physics Letters has no page charges.

For a full and complete Instructions to Authors, please refer to Chemical Physics Letters, Vol. 288, Nos. 5,6, pp. 905–906. The instructions can also be found on the World Wide Web: access under http://www.elsevier.nl or http://www.elsevier.com.

The paper used in this publication meets the requirements of ANSI/NISO Z39.48-1992 (Permanence of Paper)

Three-body Effects in Calcium(II)-ammonia Solutions: Molecular Dynamics Simulations

Wiwat Sidhisoradej, Supot Hannongbua^a, and David Ruffolo

Department of Physics (* Department of Chemistry), Faculty of Science, Chulalongkorn University, Bangkok 10330, Thailand

Z. Naturforsch. 53a, 208-216 (1998); received February 16, 1998

Molecular dynamics simulations have been performed with and without three-body corrections at an average temperature of 240 K using a flexible ammonia model. The system consists of one calcium ion and 215 ammonia molecules. The calcium(II)-ammonia interactions were newly developed, based on ab initio calculations with a basis set of double zeta quality. The role of three-body interactions on the structural and dynamical properties of the solution has been investigated. The presence of three-body corrections leads to the reduction of the first shell coordination number of Ca(II) in liquid ammonia from 9 to 8, the increase of the size of the solvation shell by 0.33 Å and the disappearance of the second solvation shell.

1. Antroduction

It has been known since the early 1940s that manybody effects can have an important influence on the results obtained from computer simulations. This can lead to a serious modification of the simulation models, especially in cases of condensed-phase systems [1]. In 1962, in order to simplify the calculation of many-body exchange effects, Jansen [2] introduced the Gaussian effective electron model and found that first-order three-body exchange effects for the rare gases could change the exchange energies by as much as 20% of the two-body exchange energies. Furthermore, Lombardi and Jansen [3] also extended the approach to four-body interactions and found that these effects were negligible for most geometries of interest. These observations have been illustrated for a monatomic gas [4] and numerous cases of ions in aqueous solution [5-8]. In addition, recent studies of Na(I), Mg(II), or Zn(II) solvation in liquid ammonia by Monte Carlo simulations showed that the three-body corrections reduce their first shell coordination number from 9 to 8, 10 to 6, or 9 to 6, respectively (9-10). Ab initio calculations with double zeta quality basis sets for the corresponding octahedral ion-ammonia complexes showed that the error in the two-body approximation of the binding energy was 17%, 30%, or 18%, respectively. However, similar investigations for Li(I) in liquid ammonia [11] showed that adding three-body corrections did not influence the first shell coordination number of 6, even though the pair approximation

Reprint requests to Dr. S. Hannongbua, Fax: (662) 2571 30.

overestimated the octahedral Li(NH₃)₆ complex binding energy by 23%.

In the present work, the role of three-body effects on the structural and dynamical properties of a Ca(II)-ammonia solution has been analyzed using the molecular dynamics method. Two simulations have been performed, with and without three-body correction functions, using newly developed Ca(II)-NH₃ pair potential and NH₃-Ca(II)-NH₃ three-body correction functions.

2. Details of the Calculations

2.1 Development of the Ca(II)-NH3 Pair Potential

To cover a range of NH₃ distances and orientations relative to Ca(II), more than 1700 Ca(II)-NH₃ pair configurations were generated. The experimental gas phase geometry of the ammonia molecule, with an N-H distance of 1.0124 Å and HNH angle of 106.67°, was taken from the literature [12] and kept constant throughout. The pair interaction energies were computed using ab intitio self-consistent fiend (SCF) calculations with double zeta quality basis sets including polarization functions, and were fitted to an analytical function of the form

$$\Delta E_{2b \, \text{fit}} = \sum_{i=1}^{4} \left[\frac{a_i}{r_i^3} + \frac{b_i}{r_i^3} + c_i \, \exp(-d_i \, r_i) + \frac{332.15 \, q_i \, q_{\text{Ca}}}{r_i} \right]. (1)$$

where $\Delta E_{2b\,\text{fit}}$ is the fitted energy in kcal·mol⁻¹, a_i, b_i, c_i , and d_i are the fitting parameters, r_i is the distance in Å

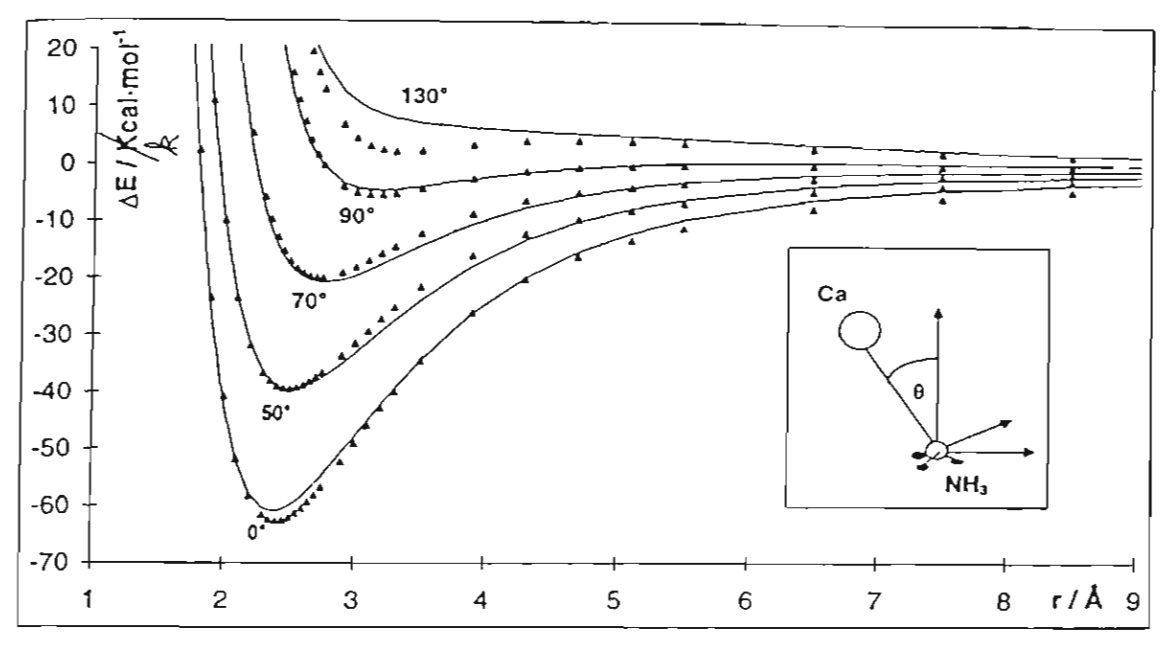


Fig. 1. Ca(II)-NH₃ dimer interaction energies (kcal·mol⁻¹) from ab initio calculations (triangles) and from best-fit pair potential functions (solid lines).

Table 1. Optimized parameters a, b, c, and d of the analytical pair potential function along with q values (in atomic units) derived from the ab initio calculations (see text for details).

	a (kcal·Å⁴·mol⁻¹)	$b = (kcal \cdot \mathring{A}^3 \cdot mol^{-1})$	c (kcal·mol ^{-t})	<i>d</i> (Å⁻¹)	q
Ca-N	3614.1584	-768.5588	-1083.0971		-0.8340
Ca-H	405.7155	173.4295	-3051.4211		0.2780

between the *i*-th atom of the ammonia molecule and the calcium ion, and q_i and q_{Ca} are their corresponding atomic net charges obtained from a Mulliken population analysis [13] in the SCF calculations. The final values of the fitting parameters for the Ca(II)-NH₃ pair potential, using a non-linear least squares fitting method, are given in Table 1. The SCF and the fitted energies for some trajectories, including the most favourable configuration where the dipole moment of the ammonia molecule points away from the ion, are compared in Figure 1.

2.2 Development of the NH₃-Ca(II)-NH₃ Three-body Correction Function

As illustrated in Figure 2, for three-body calculations, the nitrogen atom of the first ammonia molecule, N1, was at the origin of the coordinate system, and the calcium on was along the z-axis at a distance r_1 from N1. The ni

trogen atom of the second ammonia molecule, N2, was placed at the coordinates (r_2, θ_2, ϕ_2) . Both ammonia molecules are in the configuration in which their dipole vectors point to the calcium ion. The four parameters were varied independently in the ranges $1.9 \text{ Å} \le r_i \le 10.0 \text{ Å}$, $0^{\circ} \le \theta_2 \le 180^{\circ}$, and $0^{\circ} \le \phi_2 \le 60^{\circ}$ in order to cover the whole spatial configuration of the NH₃-Ca(II)-NH₃ complex. Then the three-body interaction energy, ΔE_{3b} , for each configuration was computed from the SCF energies of the monomer, dimer, and trimer according to the equation:

$$\Delta E_{sb} = \{ E\{ML_1L_2\} - E\{M\} - E\{L_1\} - E\{L_2\} \}$$

$$-\{ E\{ML_1\} - E\{M\} - E\{L_1\} \}$$

$$-\{ E\{ML_2\} - E\{M\} - E\{L_2\} \}$$

$$-\{ E\{L_1L_2\} - E\{L_1\} - E\{L_2\} \} ,$$
(2)

where M, L_1 , and L_2 denote the calcium ion and the first and second ammonia molecules, respectively. The three-body interaction energy was fitted using an analytical function of the form

$$\Delta E_{3h \, \text{fit}} = \{ R_1(r_1) R_2(r_2) + R_1(r_2) R_2(r_1) \} \ \Theta(\theta), (3)$$

where

$$R_1(r_1) = (a_0^{(1)} + a_1^{(1)}r_1 + a_2^{(1)}r_1^2 + a_3^{(1)}r_1^3) \exp(-c_1^{(1)}r_1),$$

$$\alpha_2(r_2) = (a_0^{(2)} + a_1^{(2)}r_2 + a_2^{(2)}r_2^2 + a_3^{(2)}r_2^3) \exp(-c_1^{(2)}r_2),$$

$$\Theta(\theta) = (a_0^{(3)} + a_1^{(3)}\cos\theta + a_2^{(3)}\cos^2\theta + a_3^{(3)}\cos^2\theta)$$

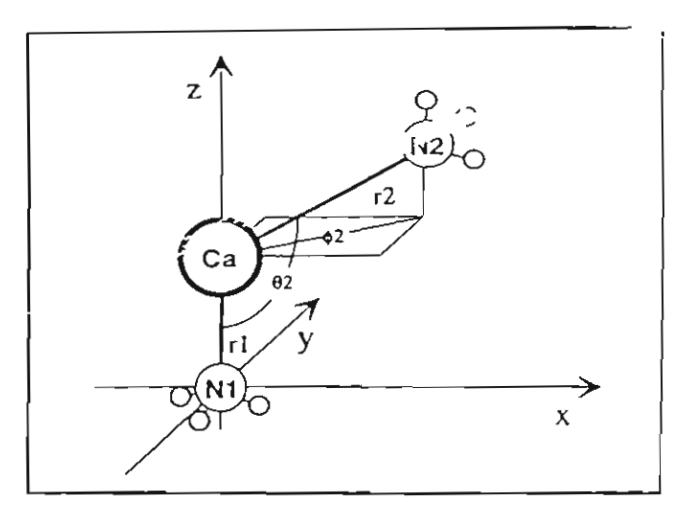


Fig. 2. Geometry for the evaluation of the NH_3 -Ca(II)- NH_3 potential for SCF calculations and the three-body correction function.

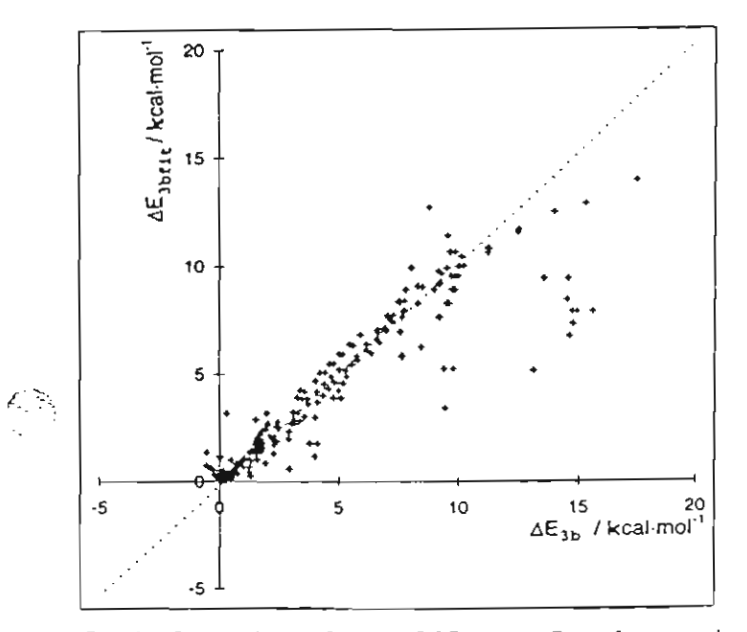


Fig. 3. Comparison of ΔE_{3b} (SCF) and $\Delta E_{3b\, fit}$ for a random sample of the generated configurations.

were employed, where $a_i^{(r)}$ and $c_j^{(r)}$ are fitting constants and θ is the N₁-Ca(II)-N₂ angle. The optimal values of the parameters are given in Table 2 while the SCF and fitted energies are compared in Figure 3. Three-dimensional plots of $\Delta E_{3h \, \text{fit}}$, r_2 and θ in the configuration shown in Fig. 2 at r_1 =1.5 Å, 2.0 Å, 2.5 Å and 3.0 Å are displayed in Figure 4.

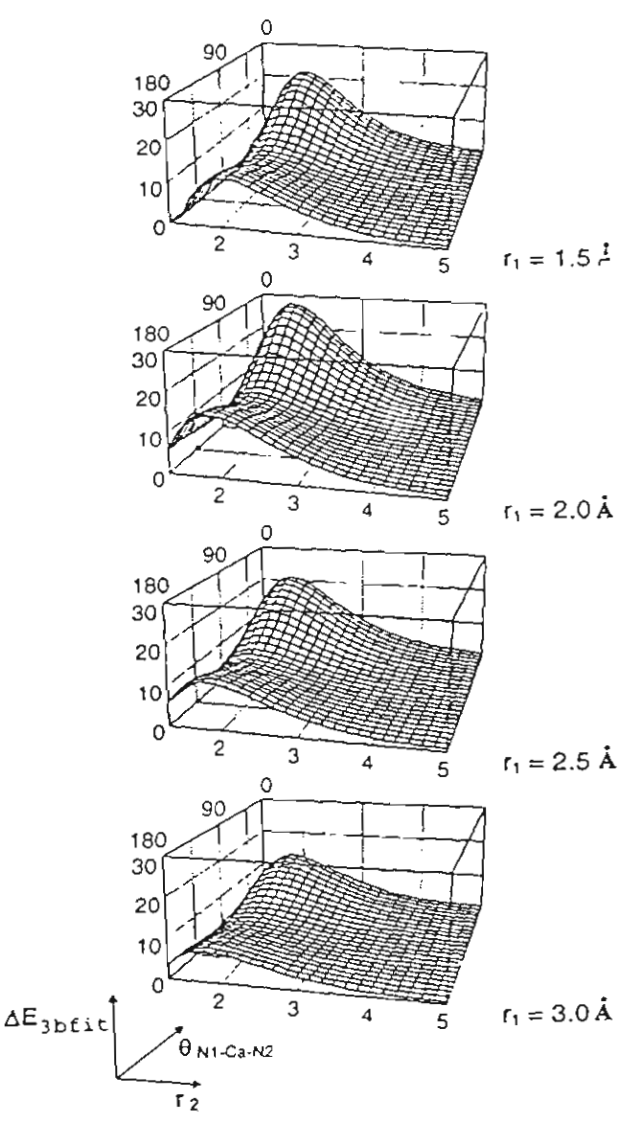


Fig. 4. Potential energy surface for the three body effect $(\Delta E_{36711}$ in kcal-mol⁻¹) in the NH₃-Ca(II)-NH₃ complex as a function of the N2-Ca(II) distance $(r_2 \text{ in } A)$ and N1-Ca(II)-N2 angle $(\theta \text{ in degrees})$ at constant N1-Ca(II) distance, $r_1 = 1.5, 2.0, 2.5, \text{ and } 3.0 \text{ Å}$ (see Figure 2).

Table 2. Optimized parameters $a_i^{(r)}$ and $c_i^{(r)}$ of the analytical 3-body correction functions (r in A and interaction energies in keal-mol⁻¹).

	;= i	i=1	i = 1
IG	-26.1335	26.7764	1.8751
(6) (1)	-0.0166	-29.0045	0.8993
	0.4367	8.4738	1.8335
2,,,	0.0303	-4).7836	-0.1777
(a) 2 (a) 3 (a)	0.7031	1.0089	~

2.3 Molecular Dynamics Simulations

For the molecular dynamics simulations, a flexible model of ammonia was employed. Both inter- and intramolecular potentials of ammonia molecules, which are the same as those used in [9-11, 14-16], were taken from [17, 18]. Two molecular dynamics simulations were performed for an average temperature of 240 K and atmospheric pressure. We used the experimental density of liquid ammonia at the simulated temperature and pressure of 0.688 g/cm³ [19], so a cube containing one calcium ion and 215 ammonia molecules has edges of length 20.67 Å. A periodic boundary condition was used, and the shifted force method [20] was employed to make short-range interactions vanish smoothly at the half-box length. The simulations were started from random configurations and were equilibrated for 10,000 time steps. Then they were continued for 80,000 time steps, corresponding to 10 picoseconds, with system configurations collected after every 10 time step. The calculations were performed on the workstations of the Austrian-Thai Center for Computer Assisted Chemical Education and Research and the National Electronic and Computer Technology Center, Bangkok, Thailand.

3. Results and Discussion

3.1 The Two- and Three-body Potential Functions

Figure 1 indicates good agreement between the SCF two-body and fitted energies, using the parameters given in Table 1. The optimal Ca(II)-N distance and the corresponding SCF energy for the most favourable configuration are 2.41 Å and -62.6 kcal·mol⁻¹, respectively.

The quality of the fit to the three-body correction energies is shown in Figure 3, where the SCF and fit energies are compared. Changes $\Delta E_{3b\,fit}$ with the distance between Ca(II) and the two nitrogen atoms, r_1 and r_2 , and of the angle between them, θ , can be clearly seen from Figure 4. Three-body effects are strong only when the two ammonia molecules are closer than 3 Å from Ca(H), and are negligible when the distance is greater than about 5 Å. All plots in Fig. 4 show two maxima near $r_2 = r_{op}$ and θ =0° or 180° and a saddle point near r_2 = r_{op} and θ =90°, where r_{op} denotes the optimal Ca(II)-N distance in the Ca(II)-NI: pair potential. In addition, the threebody energy at $\theta=0^{\circ}$ shows strongest repulsion, and the thre pody energy at $\theta = 180^{\circ}$ is about two times greater coan that at $\theta = 90^{\circ}$. The strongest interaction, for $r_2 = r_{\rm op}$ and θ =0°, where the two Ca(II)-N vectors are parallel,

cannot occur in the solution. It is interesting to note that among the plots in Fig. 4, the one with $r_1 = 2.0$ Å shows the strongest three-body effects. Note also that the three-body correction energies involve only the ammonia molecules in the first solvation shell of Ca(II). In practice, the strongest repulsive effect will be near $r_1 = r_2 = r_{\rm op}$ and $\theta = 180^{\circ}$. The corresponding value of ΔE_{3h} is about 10 kcal·mol^{-1} . This is about 20% of the most negative interaction in the Ca(II)-NH₃ pair potential at the same distances.

3.2 Structural Properties of the Solution

Ion-solvent Structure

The solvation structure of the solution can be analyzed from the radial distribution functions (RDFs) of pairs of all species involved in the solution. The Ca-N and Ca-H RDFs as well as the corresponding integration numbers obtained for each simulation are calculated and compared in Figs. Sa and Sb, respectively.

Without the three-body correction, the Ca-N RDF shows the first sharp peak centered at 2.53 Å. The integration number up to the first minimum of 3.25 Å is exactly 9. With the three-body correction, the first peak shifts to 2.86 Å, the first minimum is at 3.98 Å and the first shell coordination number reduces to 8. It is interesting to note that the shift of the first peak position by 0.33 Å in this study is much higher than the increase by 0.12 Å for Mg(II) [9] and the decrease by 0.08 Å for Zn(II) [10] in liquid ammonia. The significant increase of the size of the first solvation shell for Ca(II) can be understood in terms of the looser binding of the solvent molecules in the bigger solvation sphere for Ca(11) $(r_{op}=2.41 \text{ Å} \text{ and the corresponding stabilization energy,}$ $\Delta E_{so} = -62.6 \text{ kcal mol}^{-1}$) as compared with Mg(II) $(r_{\rm op} = 2.06 \text{ Å}, \Delta E_{\rm op} = -95.7 \text{ kcal mol}^{-1})$ and Zn(11) $(r_{op}=1.95 \text{ Å}, \Delta E_{op}=-94.1 \text{ kcal mol}^{-1})$ [9, 10]. On the other hand, it was found that the calculated size of the first solvation sphere for singly charged Li(I) and Na(I) in ammonia remains unchanged when the three-body corrections are applied [10, 11].

The influence of the three-body corrections on the second peak of the Ca(II)-N RDF is also different from that on the other doubly charged ions, Mg(II) and Zn(II). As a consequence of the loosely bound solvation sphere of Ca(II), the three-body effect causes the disappearance of a well recognized second peak of the Ca(II) in RDF, while this effect for Mg(II) and Zn(II) in us to a slight shift of the second peak to longer meances.

The Ca(II) H RDFs of simulations with and without three-body corrections show a sharp first peak at 3.39 Å :3.3.10 Å containing 27 and 24 hydrogen atoms, respectively. Changes due to the three-body corrections are

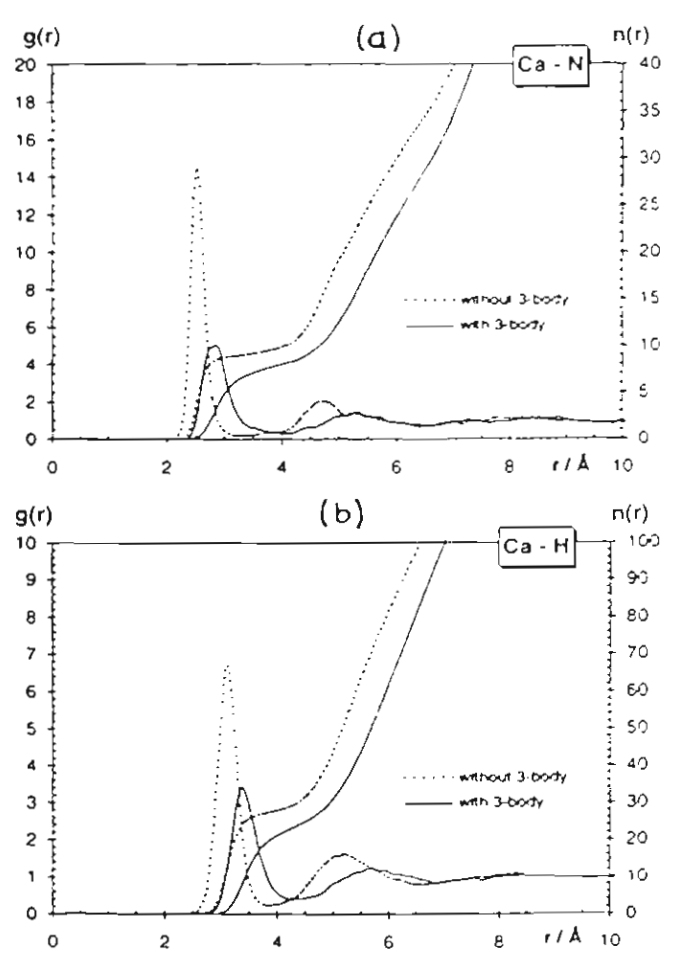


Fig. 5. Ca(II)-N and Ca(II)-H radial distribution functions and corresponding running integration numbers for simulations without and with three-body corrections.

similar to those for the Ca(II)-N RDF. As expected, no significant difference has been detected between the N-N, N-H and H-H RDFs of the two runs. Their characteristics, as well as those of the Ca(II) is and Ca(II)-H RDFs have been summarized in Table 3.

To monitor the short-range structure of the 9 (8) ammonia molecules in the first solvation shell for simulations without (with) three-body corrections, we examine the configuration-averaged distribution of the N-Ca-N angle for pairs of solvent molecules in the first shell (Figure 6). Note that the optimal spacing of 8 solvent molecules equidistant from the solute would give rise to a cubic configuration. With respect to a given solvent molecule, 3 other molecules would be at an N-Ca(II)-N angle of 70.5°, another 3 at 109.5°, and 1 at 180°; the cosines of these angles are 1/3, -1/3, and -1, respectively. The simulation results without three-body corrections show a sharp peak centered close to 1/3 and a large gap between that peak and a further peak ($\cos \alpha \cong 1/3$), indicating a cubic structure that is distorted to accommodate a ninth molecule. When three-body corrections are included, the distribution is qualitatively similar, but the peaks are much broader, indicating that the expected structure of the 8 ammonia molecules in the first solvation shell is a less rigid, time-varying, distorted cubic configuration.

Figure 7 shows the distribution of $\cos\beta$ which is defined as the angle between the vector pointing from the calcium ion to the nitrogen atom and the dipole vector for an ammonia molecule located in the first solvation shell. The distributions obtained from both simulations are sharply peaked at $\cos\beta=1.0$, with no significant difference between them. The distribution for Ca(II) is broader than that for Mg(II) and narrower relative to that of Na(I) [9]. This can be understood in terms of the strength of the interaction energy, $-\mu E \cos\beta$, between the ammonia dipole moment, μ , and the ion's electric

Table 3. Characteristics of radial distribution functions of Ca(II). $R_n r_{Mi}$, and r_{mi} are the distances in Å where for the *i*-th time $g_{\alpha\beta}(r)$ is unity, maximized, and minimized, respectively, and $n_{\alpha\beta}(r_{m1})$ is the running integration number up to r_{m1} .

	 αβ	R ₁	r _{M1}	Sap(rMI)	R_2	r_{m1}	$g_{\alpha\beta}(r_{m1})$	r_{M2}	$g_{\alpha\beta}(r_{M2})$	$n_{\alpha\beta}(r_{m1})$
without 3-body corrections	N N N H H H Ca N Ca H	2.97 2.94 3.10 2.28 2.79	3.30 3.64 3.69 2.53 3.10	2 0 1.2 1.1 15.1 6.8	4.22 4.44 4.51 2.88 3.47	5.07 5.12 5.21 3.25 3.85	0.8 0.9 0.9 0.2 0.2	6.52 6.53 6.68 4.75 5.25	1.1 1.1 1.0 2 1 1.6	12.6 39.1 41.1 8.97 27.4
with 3-body corrections	N N N H H H Ca N Ca H	2.99 2.97 3.08 2.51 3.08	3.34 3.67 3.81 2.86 3.39	2, } 1, 2 1, 1 5 + 3, 4	4.25 4.49 4.55 3.30 3.81	5.13 5.02 5.37 3.98 4.42	0.7 0.9 0.9 0.3 0.4	6.60 6.69 6.73 5.28 5.68	1.1 1.0 1.5 1.2	12.8 36.8 44.8 8.19 24.3

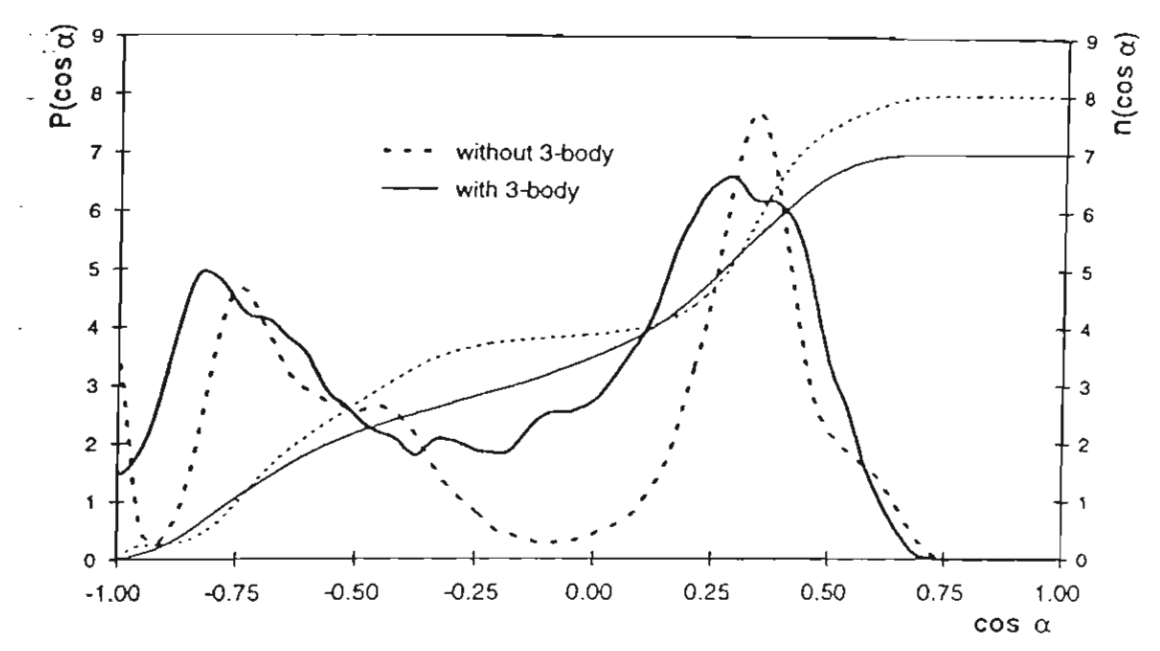


Fig. 6. Distribution of the cosine of the N-Ca(II)-N angle, $p(\cos\alpha)$, for a pair of ammonia molecules in the first solvation sphere and running integration number, $n(\cos\alpha)$.

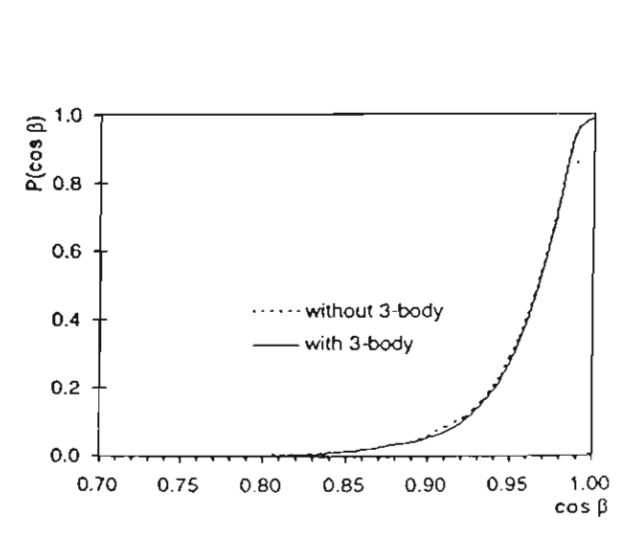


Fig. 7. Distribution of $\cos \beta$ for ammonia molecules in the first solvation shell of calcium ion (see text for details).

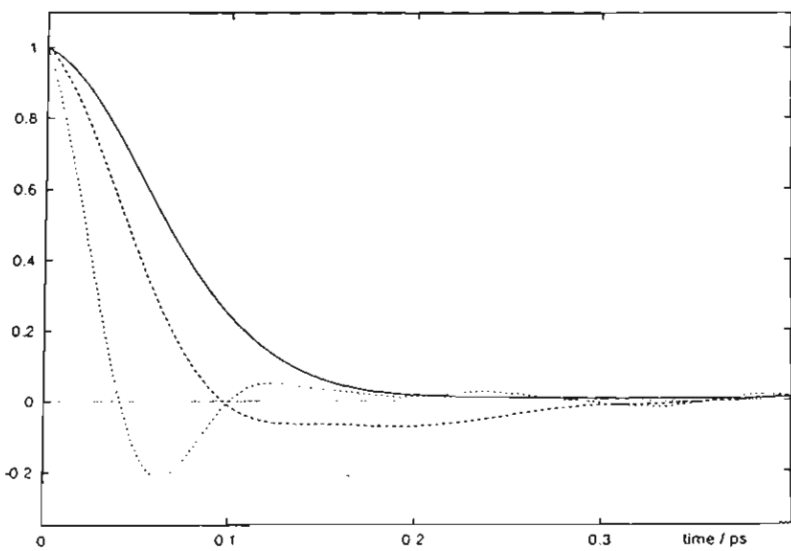


Fig. 8. Normalized center of mass velocity autocorrelation functions for ammonia molecules in the bulk (solid line) and the first solvation shell of Ca(II) obtained from our simulations with (long-dashed line) and without (short-dashed line) three-body corrections.

field, $E \approx q/r^2$. Based on our simulations, the strength of the electric field at the first solvation shell is in the order Mg(II)>Ca(II)>Na(I): this explains why Mg(II) has the narrowest $\cos \beta$ distribution and Na(I) has the broadest.

3.3 Dynamical Properties of the Solution

Translational Motions

Translational motions of the molecules can be represented by the velocity autocorrelation function (acf). The center-of-mass acfs of the two simulations, with and

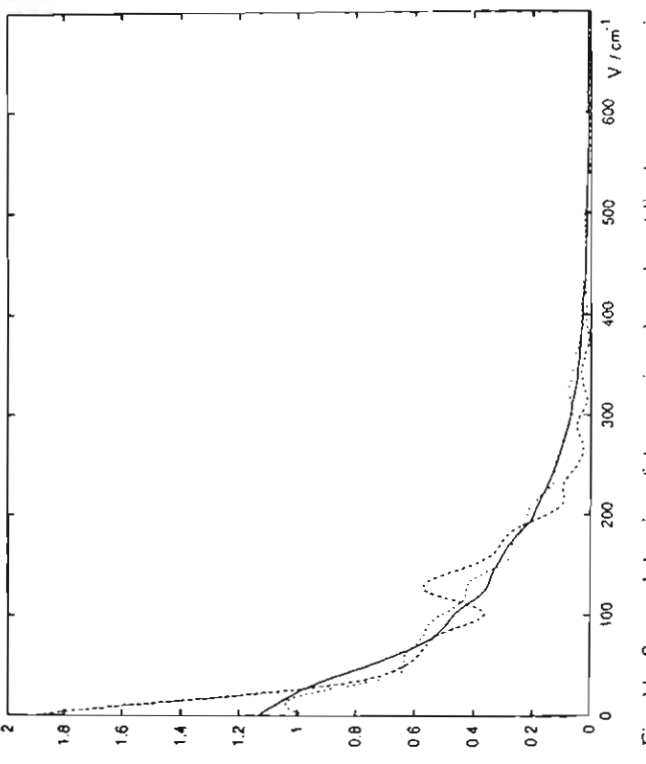


Fig. 11. Spectral density of the rotation about the τ (dipole moment) axis for the molecules as defined in Figure 10.

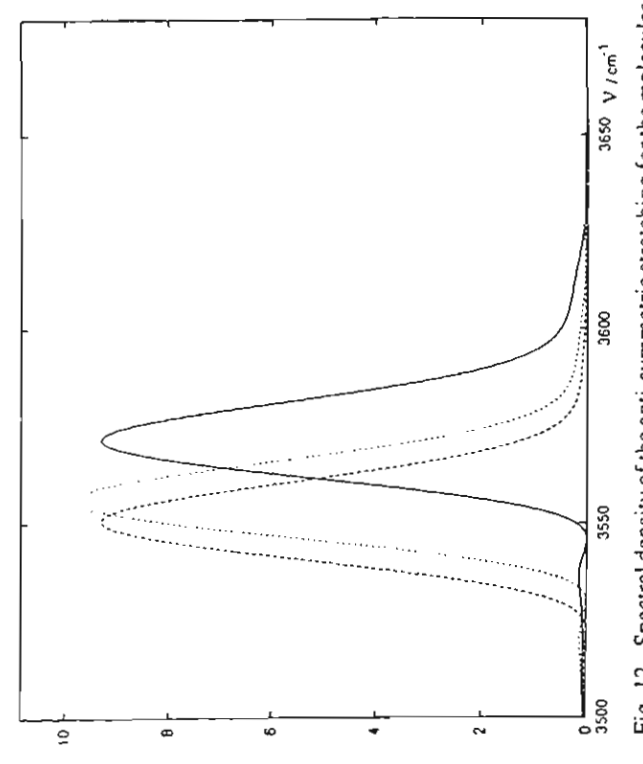


Fig. 12. Spectral density of the anti-symmetric stretching for the molecules as defined in Figure 10.

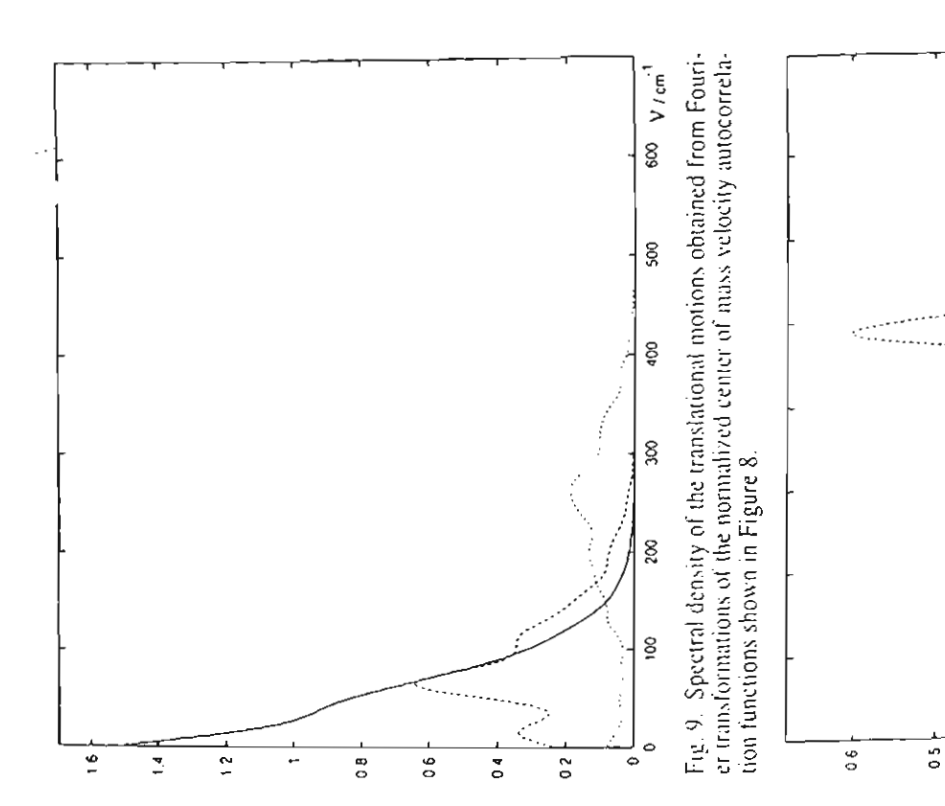


Fig. 10. Spectral density of the rotation about the x axis (defined by the configuration of the first ammonia molecule in Fig. 2) for ammonia molecules in the bulk (solid line) and the first solvation shell of Ca(II) obtained from our simulations with (long-dash line) and without (short-dash line) three-body corrections.

700 V /cm⁻¹

8

0 5

9 4

03

-

without the three-body corrections, both for molecules in the bulk and the first solvation shell, have been calculated separately and plotted in Figure 8. Fourier transform, $\Im(\omega)$, is called the spectral density and is defined

$$\Im(\omega) = \int_{0}^{\infty} C_{\nu}(t) \cos(\omega t) dt, \qquad (4)$$

where $C_{\nu}(t)$ denotes the acfs (Figure 9).

The acfs for bulk molecules decay smoothly to zero at about 0.25 ps for both runs. The acf for molecules in the first solvation shell for the simulation, using only the pair potentials, crosses zero at 0.038 ps before overshooting due to a restoring force, which is much faster than the time of 0.086 ps when the three-body effects are included. The spectral densities of the three types of molecules (bulk, first solvation shell with three-body correction and first solvation shell using only pair potentials) peak at 0, 67 and 259 cm⁻¹, respectively (Figure 9). We see that bulk molecules can translate freely (with zero frequency), while solvated molecules are bound more tightly when the three-body corrections are neglected. In conclusion, the acf and spectral density plots confirm that the three-body corrections yield looser binding of the solvated molecules.

It is found experimentally that the self-diffusion coefficient (D) of liquid ammonia is strongly temperature dependent [21], and it is not yet possible to model that properly using simulation data [18, 22]. A self-diffusion coefficient for bulk ammonia calculated in our previous work [18] using the same NH3-NH3 pair potential as in this study, and calculated in [22] are approximately 70% too high and 80% too low, respectively, compared with the experimental value at 277 K [21, 23]. However, for the ammonia molecules in the first solvation shell of Ca(II) we obtained $D = (3.80 \pm 2.22) \times 10^{-4} \text{ cm}^2 \text{ s}^{-1}$ and $D=(5.75\pm2.35)\times10^{-5}$ cm² s⁻¹ for the simulations with and without three-body corrections, respectively. The relatively large error is due to the fact that there are only a few ammonia molecules involved in the statistical calculations.

Librational Motions

Librational dynamics of the ammonia molecules in the simulated system can be studied through the Fourier transform of the act of velocity components of hydrogen atoms. Details of the projections of the velocities onto degenerate axes are explained in [24]. The spectral dia-

Table 4. Comparison of vibrational frequencies (cm⁻¹) from our simulations and experimental results.

Mode	Ca(II)-NH	simulations	Pure ammonia experimental data		
	solvation	bulk	liquid	gas	
	shell	liquid	(25)	[17]	
Sym. Bend.	1310	1184	1066	932,968	
Asym. Bend	1560	1643	1638	1627	
Sym. Stretch.	3251	3418	3240	3336	
Asym. Stretch.	3557	3580	3379	3444	

grams of rotation around x and z axes, defined by the configuration of the first ammonia molecule (NI) in Fig. 2, are shown in Figs. 10 and 11, respectively.

The rotational spectrum around the x axis of the molecules in the bulk peaks near 200 cm⁻¹, while those of solvated molecules for both simulations, with and without three-body corrections are strong between 400 cm⁻¹ to 600 cm⁻¹. The Fourier transforms of the acfs for rotation about the dipole moment axis (Fig. 11) are all quite similar. The maximum at zero frequency indicates fairly free rotation around that axis.

Vibrational Motions

Table 4 shows the consistency between the vibrational frequencies from experiments and from simulations, especially between liquid ammonia and bulk molecules in simulations. From the qualitative agreement in the bulk system, it can be expected that the potentials employed in the simulation lead to a qualitatively correct description of the effect of the calcium ion. The blueshift of the symmetric bending and redshift of the symmetric stretching mode for the molecules in the solvation shell indicates the influence of calcium ion interactions on the ammonia molecules. Similar effects were also found in the system of Li⁺ in liquid ammonia [18] and systems of K⁺ and I" in liquid ammonia [14]. The effect of adding threebody corrections on these frequencies was not strong, except for a slightly decreasing shift in the anti-symmetric stretching mode, as shown in Figure 12.

Acknowledgement

Financial support by the Thailand Research Fund and the generous supply of computer time by the Austrian-Thai Center for Computer Assisted Chemical Education and Research in Bangkok and the National Electronic and Computer Technology, Center, Bangkok, Thailand are gratefully acknowledged

- [1] M. J. Elrod and R. J. Saykally, Chem. Rev. 94, 1975 (1994).
- [2] L. Jansen, Phys. Rev. 125, 1798 (1962).
- [3] E. Lombardi and L. Jansen, Phys. Rev. 167, 822 (1968).
- [4] E. E. Polymeropoulos and J. Brickmann, Chem. Phys.
- Lett. 92, 59 (1982).
 [5] J. Kim, S. Lee, S. J. Cho, B. J. Mhin, and K. S. Kin, J. Chem. Phys. 102, 839 (1995).
 [6] T. Lybrand and P. A. Kollman, J. Chem. Phys. 83, 2923
- (1985).
- [7] R. Kelterbaum, N. Turki, A. Rahmouni, and E. Kochanski, J. Chem. Phys. 100, 1589 (1944).

- [8] L. X. Dang, J. Chem. Phys. 96, 6970 (1992). [9] S. Hannongbua, J. Chem. Phys. 106, 6076 (1997). [10] S. Hannongbua, T. Kerdcharoen, and B. M. Rode, J. Chem. Phys. 96, 6945 (1992).
- [11] S. Hannongbua, Chem. Phys. Lett. (1998) in press.[12] W. S. Benedict and E. K. Plyler, Can. J. Phys. 35, 890 (1985).
- [13] R. S. Mulliken, J. Chem. Phys. 23, 1833, 1841, 2338, 2343 (1955).

- [14] A. Tongraar, S. Hannongbua, and B. M. Rode, Chem. Phys. 219, 279 (1997).
- [15] S. Hannongbua, Aust. J. Chem. 44, 447 (1991)
- [16] S. Hannongbua and B. M. Rode, Chem. Phys. 162, 257 (1992).
- [17] V. Spirko, J. Mol. Spectrosc. 101, 30 (1983).[18] S. Hannongbua, T. Ishida, E. Spohr, and K. Heinzenger, Z. Naturforsch. 43a, 572 (1988).
- [19] R. C. Weast, Handbook of Chemistry and Physics, 57th ed.; CRC: Ohio 1976–1977.
- [20] W. B. Streett, D. J. Tildeslay, and G. Saville, ACS Symp. Ser. 86, 144 (1978).
- [21] A. N. Garroway and R. M. Cotts, Phys. Rev. A7, 635 (1973)
- [22] R. W. Impey and M. L. Klein, Chem. Phys. Lett. 104, 579 (1984)
- [23] D. E. O'Reilly, E. M. Peterson, and C. E. Scheie, J. Chem. Phys. 58, 4072 (1973).
- [24] P. Bopp, Chem. Phys. 196, 205 (1986).
- [25] T. Birchall, I. Drummond, J. Chem. Soc. 1970, 1859.

The Best Structural Data of Liquid Ammonia based on the Pair Approximation: First Principle Monte Carlo Simulation

by

Supot Hannongbua

Chemistry Department, Faculty of Science, Chulalongkorn University,

Bangkok 10330, THAILAND (supot@atc.atccu.chula.ac.th)

Abstract

Monte Carlo simulations have been performed for liquid ammonia at 277 K and 1 atm with and without the pair potentials. The NH₃-NH₃ potential function used in the first simulation has been developed based on *ab initio* calculations with TZP (Triple Zeta plus Polarization function) basis sets. For the second run without the pair potential, the pair interactions have been calculated directly during the simulation using the first principle *ab initio* method with the same basis sets. The nitrogen-nitrogen radial distribution function (RDF) obtained from the later case which is considered as the best structural data based on the pair approximation, shows a sharp first peak at 3.4 Å followed by a broad shoulder ranging from 4.2 Å to 4.8 Å. This shoulder has been observed for the first time, theoretically, unless that reported experimentally at 3.7 Å. In addition, energetic error due to three-body effects have been clearly visualized. Its effects on the N-N RDF at short distance has been consistently detected. Sensitivity of the structural properties of the solution to the intermolecular, both pair and three-body, interactions has been extensively discussed.

1. Introduction

Since the first experimental report on the structural data of liquid ammonia by Narten in 1976 (1), in terms of nitrogen-nitrogen radial distribution function (RDF) which shows a sharp first peak at 3.4 Å and pronounce shoulder at 3.7 Å. Several attempts have been made (2-9), theoretically, to reproduce the experimental N-N RDF, but no entirely satisfactory model has yet emerged. Discrepancy took place concerning an appearance of the RDF shoulder.

There is no way to ascertain, on the basis of existing data, whether the N-N RDF is caused primarily by an error due to the diffraction measurement or the development of the pair potential as both processes are so complicate. To examine this problem, structural property of liquid ammonia has been evaluated using Monte Carlo technique. Simulations have been performed based on the pair approximations with and without pair potential. In the second run, interaction between the two ammonia molecules has been calculated directly using the first principle *ab initio* method.

2. Details of the Calculations

2.1 Development of the pair potential

To develop the NH₃-NH₃ pair potential, more than 1,500 configurations of the dimer have been generated. Their interaction energies have been calculated using an *ab initio* method with TZP (Triple Zeta plus Polarization function) basis sets (10). The data points were, then, fitted to analytical function. The final form of the fitted function with the optimal parameters is:

$$\Delta E(L,A) = \sum_{i=1}^{4} \sum_{j=1}^{4} \frac{A_{ij}}{r_{ij}^{6}} + \frac{B_{ij}}{r_{ij}^{12}} + \frac{q_{i}q_{j}}{r_{ij}}$$
 [1],

where 4 is numbers of atom of ammonia, A_{ij} , B_{ij} are fitting constants, r_{ij} is the distance between an atom i and an atom j of the two ammonia molecules, q_i and q_j are the atomic net charges of the atom i and j in atomic units, obtained from the population analysis (11) of the isolated molecules. Figure 1, optimal configuration of the ammonia dimer has been displayed.

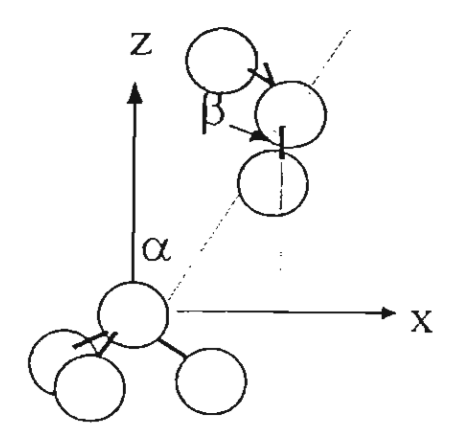


Figure 1 Optimal configuration of the ammonia dimer ($\alpha=\beta=12^{\circ}$).

2.2 Investigation of the Three body-effects

To monitor an energetic error of the pair approximation due to the three body effects, the three-body interaction energies, E_{3bd}, have been calculated for the three ammonia molecules, in the three configurations shown in Figure 2, varying 2 Å $\leq r_1$, $r_2 \le 10$ Å, where r_1 and r_2 denote distances from nitrogen atom of the central ammonia, L_c, to nitrogen atom of the first (L₁) and the second (L₂) ammonia molecules, respectively. Note that, nitrogen atoms of L₁ and L₂ lie in the configuration to form linear hydrogen bond with L_c. For the ammonia molecules which bind to the lone pair side of L_c an angle (a) between dipole vector of L_c and vector pointing from the nitrogen atom of L_c to that of the other nitrogen is 50°. This value is estimated from probability plot of the geometrical arrangement of the nearest neighbor NH₃ molecules around the central one obtained from molecular dynamics simulation of pure liquid ammonia (9). For easier monitoring, the three configurations of the trimer, where L₁ and L2 are coordinated to Lc on the lone pair, the hydrogen and the opposite sides, are and donor-acceptor configurations, named double-donor, double-acceptor respectively.

For each configuration, E_{3bd} , was computed from 13 terms of the *ab initio* energies on the right side of equation [2],

$$E_{3bd} = [E\{L_{c}L_{1}L_{2}\} - E\{L_{c}\} - E\{L_{1}\} - E\{L_{2}\}]$$

$$-[E\{L_{c}L_{1}\} - E\{L_{c}\} - E\{L_{1}\}]$$

$$-[E\{L_{c}L_{2}\} - E\{L_{c}\} - E\{L_{2}\}]$$

$$-[E\{L_{1}L_{2}\} - E\{L_{1}\} - E\{L_{2}\}]$$
[2].

All energies on the right-hand side of equation [2] are total energies of the system in brackets. For each plot, more than 400 three-body data points have been computed, using also the TZP basis sets. The results are displayed in Figure 2.

(a) (b) (c)

Figure 2 Ammonia trimer in the donor-donor (a), donor-acceptor (b) and acceptor-acceptor (c) configurations (α =50°).

2.3 Monte Carlo Simulations

Monte Carlo simulations have been performed for liquid ammonia with and without pair potentials at 277 K and 1 atm. The system consists of 202 rigid ammonia molecules. Their experimental gas phase geometry, with the N-H distance of 1.0124 Å and the H-N-H angle of 106.67°, was taken from ref. (12). For the first simulation, the NH₃-NH₃ pair potential from equation [1] which is developed based on *ab initio* calculations with TZP basis sets have been used. In the second run using the pair approximation without the pair potential which is, afterward, named first principle Monte Carlo, the pair interactions have been calculated directly by means of *ab initio* method with the same basis sets during the run. The experimental density of pure liquid ammonia at 277 K and atmospheric pressure of 0.633 g.cm⁻³ leads to the box length of the periodic cube of 20.99 Å. Cut off of the pair potentials at half of this length and at 7.0 Å were applied for the simulations with and without pair potentials, respectively.

Starting configuration of the first simulation using the pair potential was generated randomly and a further 5 million configurations after equilibration were used to evaluate structural data of the liquid. The final configuration obtained from this run was, then, used as the starting configuration for the second run without the pair

potential. To equilibrate the later system, simulation has been carried out for 40,000 configurations. Then, another 40,000 configurations have been collected for structural evaluation.

3. Results and Discussion

3.1 Dimer configuration and the pair potential

With the *ab initio* calculations using TZP basis set, the optimal stabilization energy is -2.53 kcal.mol⁻¹ taken place at the optimal N-N distance, r_{op}, of 3.4 Å. The total energy and the dipole moment of the monomer are -56.21603 Hartree and 1.87 D, respectively. The observed dimer configuration agrees well with those found using *ab initio* calculations with inclusion of correlation effects (8). Referring to the experimental dipole moment of the ammonia monomer of 1.47 D, the calculated value using the TZP basis sets is the best one, in comparison with the values obtained from the 6-31G, 6-31G*, 6-31G**, DZP and DZ2P basis sets of 2.23 D, 1.95 D, 1.89 D, 2.35 D and 1.97 D, respectively. Note that, although the STO-3G value of 1.78 D is much closer to the experimental data due to error cancellation in the SCF-LCAO-MO method but it is known that this basis sets yields a wrong configuration of the dimer.

3.2 Characteristic of the first principle simulation

Some comments should be made concerning time required for the Monte Carlo simulation using pair approximation without pair potential. Single point calculation with TZP basis sets of the ammonia dimer using G92 and G94 programs (xx) on the SGI power challenge workstation consumes 30 - 35 seconds, CPU time. Within a spherical cut off of 7.0 Å around central ammonia, interactions with about 30 neighbor molecules have to be calculated, i.e., each move of the first principle Monte Carlo takes approximately 20 mins. Therefore, total CPU time for the 80,000 moves of this study is about 3 years. Cut off of the dimer interaction at 7.0 Å applied for this simulation is necessary in order to make this work possible, i.e., this event helps to reduce the CPU time by a factor of three, in comparison with that cut off at half of the box length. In addition, the pair NH₃-NH₃ interaction in the most favorable configuration of the dimer is almost disappear beyond 5-6 Å.

3.3 Nitrogen-nitrogen radial distribution functions

Figure 3, N-N radial distribution functions obtained from the simulations with and without pair potentials have been plotted. That observed experimentally by Narten (1) at the same temperature, 277 K, has been also given for comparison. As describe and discuss in details in ref. (9), in term of the height and the position of the first maximum as well as the first shell coordination number, the N-N RDFs obtained from the simulation using pair potential agrees well with the X-ray measurement. In consistent with the results obtained from the other theoretical works (xxs), the simulated RDF does not reproduce the experimental shoulder at 3.7 Å.

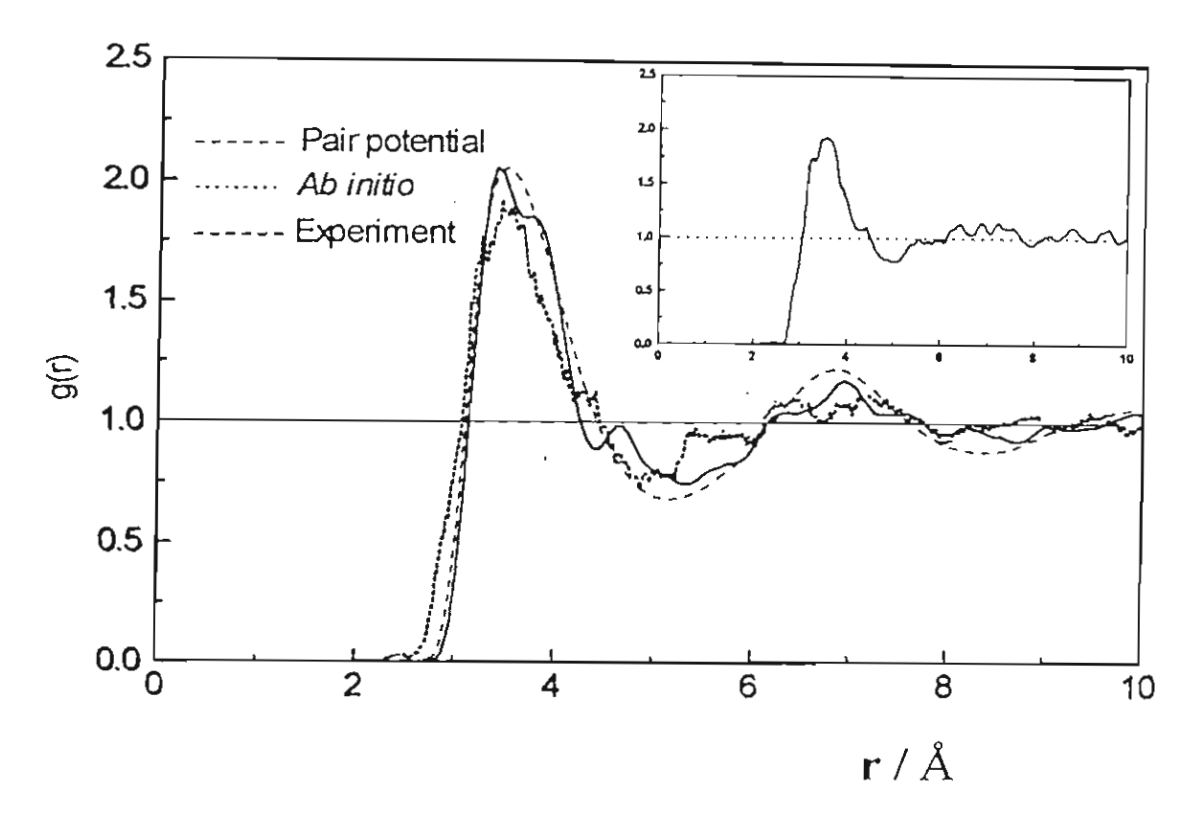


Figure 3 Nitrogen-nitrogen radial distribution functions obtained from the X-ray diffraction and from the simulations with and without pair potentials. The first principle RDF averaged from 20,000 configurations has been also given in the insert for comparison.

Due to methodical limit, very short simulation has been carried out and non-smooth of the RDFs have been yielded. However, longer simulation would have lead to better quality of the plot but would not have changed the main feature of the RDFs. To certify this statement, the N-N RDF collected from the first 20,000 configurations, after equilibration, has been evaluated and plotted in the insert of Figure 3. Similarity of the two plots, averaged from 20,000 and 40,000 configurations, indicates reliability of the first principle RDFs reported in this study.

3.3.1 Simulated N-N RDFs with and without pair potentials

The nitrogen-nitrogen radial distribution functions obtained from the first principle simulation (N-Nab RDF) which is considered as the best structural data based on the pair approximation, shows first peak at 3.4 Å (hump of the peak is within the fluctuation limit) followed by broad shoulder ranging from 4.0 Å to 4.8 Å. Unless an appear of the pronounce shoulder, significant changes of the N-Nab RDF compared to that of normal simulation using pair potential (N-N_{fit} RDF) are observed in the three regions, r < 3 Å, 3.5 Å < r < 4.0 Å and 5 Å < r < 6 Å. The distortions at r < 3 Å and 5 $\rm {\rm \AA} < r < 6 \ {\rm \AA}$ are a consequence of a poorly fit of the interaction potentials in the two regions in comparison with the ab initio data. With an assumption that those configurations don't take place in the simulation. Therefore, most author weighs the fit to the global minimum of the interaction energy of the dimer at the optimal N-N distance. This leads to discrepancies in the two regions around the minima. At $r < r_{op}$, the fitted curve is usually above the ab initio one (the fitted energies are more positive or less negative than the ab initio data) and confirms the shift of the N-Nfit RDF to shorter distance to be N-Nab RDF, i.e., the N-Nab RDF start to be detected before the N-N_{fit} RDF. For 5 Å < r < 6 Å, inconsistency between the N-N_{fit} and the N-N_{ab} RDFs could be related to the shortcoming of the pair potential in the region beyond the minima. In addition, shift of the N-N_{fit} second peak at 5 Å < r < 6 Å to shorter distance (Figure 3) can be assigned consequently to the changes at $r \le 3$ Å and 3.5 Å $\le r \le 4.0$ Å as well as the formation of the shoulder of the N-N ab RDF.

Taking into account all the above distortions, it can be conclude clearly that structural properties of the system of weak interaction such as liquid ammonia is very sensitive to the quality of the fit and requires a more complicated functions which can represent *ab initio* data in all regions. The authors must play much attention on the discrepancies of the fitted and the ab initio data in the short distance before the minima and in medium distance beyond the minima.

Strangely enough the experimental RDF at r < 3 Å is better reproduced by the N-N_{fit} RDF which is generated from the simulation using the under-estimated pair potential (fitted energies are more positive or less negative than the *ab initio* data) than the N-N_{ab} RDF. The reason for this event is assigned to the three-body effect which is known to play strong role at short distance (14-23).

Interest is centered on an appear of the pronounce shoulder of the N-N_{2b} RDF between 4.0 Å to 4.4 Å. This is observed for the first time based on theoretical approach. The difference in the RDF characters obtained from the two simulations, with and without the pair potentials, using the same levels of ab initio data, is inevitably to be assigned to the shortcoming in the fitting steps in developing of the pair potential. Source of discrepancy lies in an existing of several minima of similar stabilization energies. Some examples are the stabilization energies of -2.40, -2.53 and -2.25 kcal.mol-1 at the optimal N-N distances of 2.54 Å obtained from the dimer configurations of the two ammonia molecules shown in Figure 1 where $\alpha = 0^{\circ}$, 10° and 20°, respectively. Those configurations suppose to be taken place in the simulation, as well as in reality, as the energy differences are within thermal fluctuation at 298 K, KT= 0.6 kcal.mol⁻¹ where K denotes Boltzmann constant. Such minima can not be modeled properly by simple analytical functions. Weighing of the fit to one will lead to distortions, in term of both energy minimum and the corresponding distance, on the other minima while quality of the fit still statistically satisfy. As structural properties are sensitive to quality of the function, especially around potent minima, therefore, orientation of the molecules generated from the fitted energy surface, which contains one appropriated minimum, is inconsistent with that from the ab initio surface which contains several minima of similar well dept. The above information allows us to conclude that structural properties of the weak hydrogen bonded system is sensitive to all potent minima. Therefore, more complicated function and more attention in developing of the pair potential would have been required.

3.3.2 The experimental and the first principle N-N RDFs

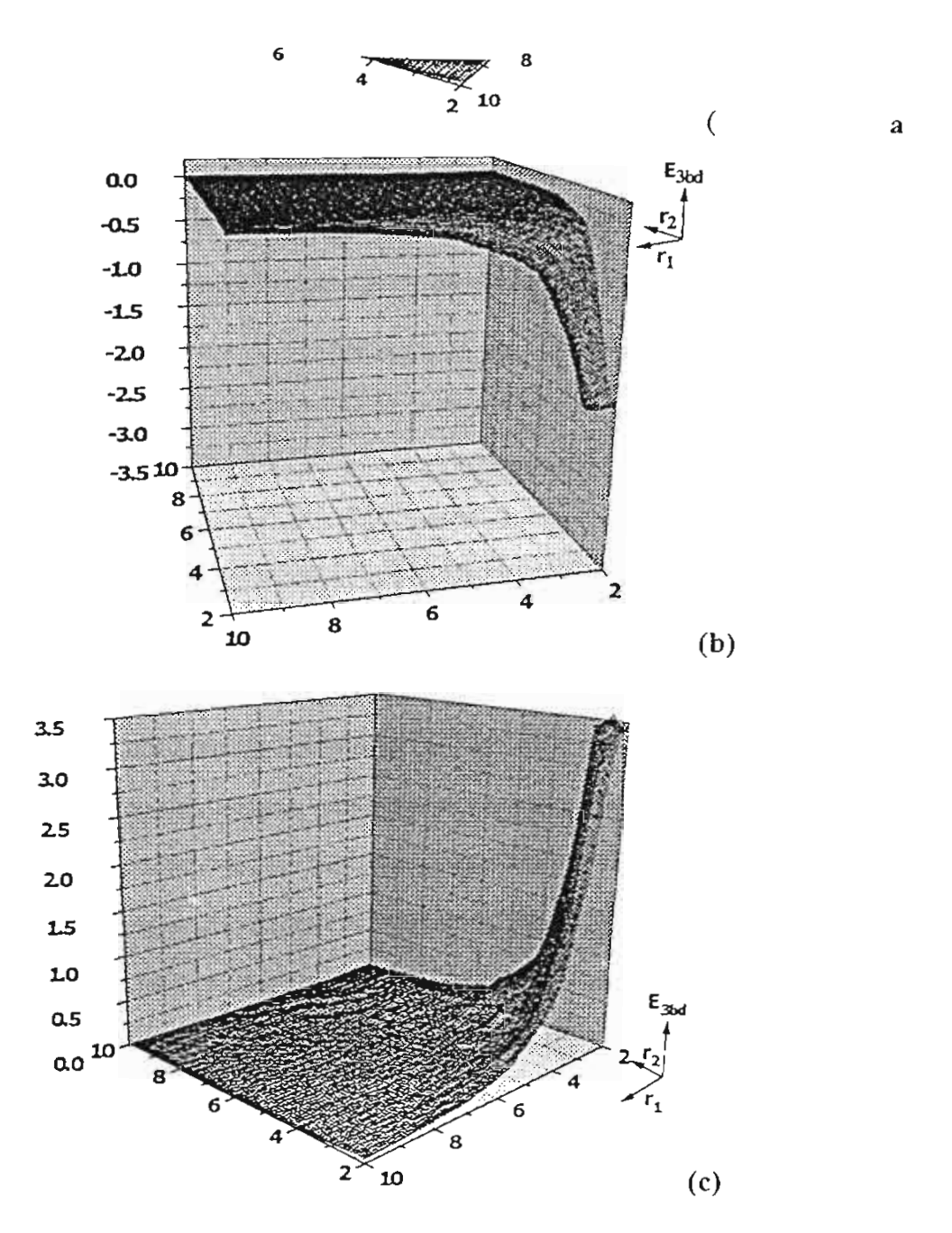


Figure 4 Three-body interaction energies for the ammonia trimer in the donor-donor (a), donor-acceptor (b) and acceptor-acceptor (c) configurations shown in Figure 2.

Compare to the X-ray structure, the N-N RDF obtained from the first principle simulation based on the pair approximation starts to be detected earlier. Its shoulder appears at longer distance and covers the X-ray shoulder centered at 4.8 Å. Its second peak starts at shorter distance and is less pronounce. An appear of the N-N_{ab} RDF which starts to be found before that of experimental one, N-N_{exp} RDF, indicates a less repulsion of the pair interaction derived from *ab initio* calculations during the simulation than that in reality, where many-body effects have been taken into account. Therefore, source of discrepancy at short distance can be, again, assigned to the

exclusion of the many-body effects in the Monte Carlo simulation. Further confirmations are discussed in detail in the next section in terms of three-body interaction energies and their orientation dependence.

3.4 Influence of the three-body effects on the N-N RDF

Figure 4a-4c, three-body interaction energies, E_{3bd} , of the three configurations shown in Figure 1a-1c have been, respectively, displayed. The E_{3bd} in the double-donor configuration (Figure 4a), E_{3bd}^{dd} , shows weak repulsive interaction with two maxima of 0.5 kcal.mol⁻¹ at $r_1 = r_{op} = 3.4$ Å, $r_2 = 2.5$ Å and at $r_1 = 2.5$ Å, $r_2 = r_{op} = 3.4$ Å. Note that, E_{3bd}^{dd} at $r_1 = r_2 = r_{op} = 3.4$ Å is 0.1 kcal.mol⁻¹. In the donor-acceptor configuration (Figure 4b), E_{3bd}^{do} is attractive and decays to zero at $r_1 = r_2 = 5.0$ Å. Although the E_{3bd}^{do} is quite strong attractive at short distance but its value at $r_1 = r_2 = r_{op} = 3.4$ Å is only -0.2 kcal.mol⁻¹. Strongest repulsion of the E_{3bd} is observed in the configuration where the two ammonia molecules coordinate to the two acceptors, hydrogen atoms, of the central ammonia, E_{3bd}^{3d} (Figure 4c). Fast decay of the E_{3bd}^{3d} leads to its value at $r_1 = r_2 = r_{op}$ of 0.7 kcal.mol⁻¹. Strong repulsion of the E_{3bd} at short distances confirms the less discrepancy of the N-N_{fit} than the N-N_{ab} RDFs in comparison with the experimental one.

4. Acknowledgment

Financial support by the Thailand Research Fund and the National Research Council of Thailand, and the generous supply of computer time by the National Electronic and Computer Technology Center, Bangkok, Thailand is gratefully acknowledged.

5. References

- 1. A. H. Narten, J. Chem. Phys. 66, 3117 (1977).
- 2. F. H. Stillinger, Israel J. Chem. 14, 130 (1975).
- 3. M. L. Klein, I. R. McDonald and R. Righini, J. Chem. Phys. 71, 3673 (1979).
- 4. W. L. Jorgensen and M. Ibrahim, J. Am. Chem. Soc. 102, 3309 (1980).
- 5. M. L. Klein and I. R. McDonald, J. Chem. Phys. 74, 4214 (1981).
- A. Hinchliffe, D. C. Bounds, M. L. Klein, I. R. McDonald and R. Righini, J. Chem. Phys. 74, 1211 (1981).

- 7. R. W. Impey and M. L. Klein, Chem. Phys. Lett. 104, 579 (1984).
- 8. K. P. Sagarik, P. Ahlrich and S. Brode, Mol. Phys. 57, 1247 (1986).
- 9. S. Hannongbua, T. Ishida, E. Spohr and K. Heinzinger, Z. Naturforsch. 43a, 572 (1988).
- 10. T. H. Dunning J. Chem. Phys. 53, 2823 (1970).
- 11. R. S. Mulliken, J. Chem. Phys. 23, 1833 (1955).
- 12. W. S. Benedict and E. K. Plyler, Can. J. Phys. 35, 890 (1985).
- 13. M. J. Frisch, G. W. Trucks, M. Head-Gordon, P. M. W. Gill, M. W. Wong, J. B. Foresman, B. G. Johnson, H. B. Schlegel, M. A. Robb, E. S. Replogle, R. Gomperts, J. L. Andres, K. Raghavachari, J. S. Binkley, C. Gonzalez, R. L. Martin, D. J. Fox, D. J. Defrees, J. Beker, J. J. P. Stewart, and J. A. Pople, Gaussian 92, Revision A (Gaussian, Inc., Pittsburgh PA, 1992).
- 14. E. Clementi, H. Kistenmacher, W. Kolos and S. Romano, *Theor. Chim. Acta* 55, 257 (1980).
- 15. H. Kistenmacher, H. Popkie and E. Clementi, J. Phys. Chem. 61, 799 1974).
- 16. M. M. Probst, Chem. Phys. Lett. 137, 229 (1987).
- 17. E. Kochanski, Chem. Phys. Lett. 132, 143 (1987).
- 18. T. P. Lybrand and P. A. Kollman, J. Chem. Phys. 88, 2923 (1985).
- 19. I. Ortega-Blake, J. Hernandez and O. Novaro, J. Chem. Phys. 81, 1894 (1984).
- 20. M. M. Szczesniak, R. A. Kendall and G. Chalasinki, J. Chem. Phys. 95, 5169 (1991).
- 21. S. Hannongbua, T. Kerdcharoen and B. M. Rode, J. Chem. Phys. 96, 6945 (1992).
- 22. S. Hannongbua, J. Chem. Phys. 106, 6076 (1997).
- 23. S. Hannongbua, Chem. Phys. Lett. 228, 663 (1998).